

RD-A159 324

WAVE MOTION ANALYSIS OF A NON-SPINNING LIQUID FILLED
CYLINDER(U) ARMY BALLISTIC RESEARCH LAB ABERDEEN
PROVING GROUND MD P WEINACHT ET AL JUN 85 BRL-MR-3451

1/1

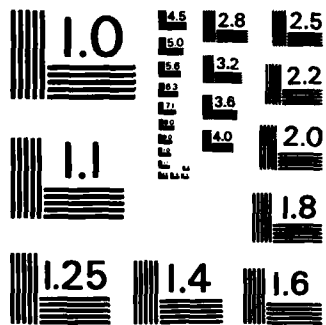
UNCLASSIFIED

F/G 19/4

NL

END

FILED
6/16



MICROCOPY RESOLUTION TEST CHART
NATIONAL BUREAU OF STANDARDS - 1963 - A

AD-A159 324

(2)



US ARMY
MATERIEL
COMMAND

AD

MEMORANDUM REPORT BRL-MR-3451

WAVE MOTION ANALYSIS OF A NON-SPINNING
LIQUID FILLED CYLINDER

Paul Weinacht
Charles J. Nietubicz

June 1985

DTIC
SELECTED
SEP 23 1985

APPROVED FOR PUBLIC RELEASE; DISTRIBUTION UNLIMITED.

US ARMY BALLISTIC RESEARCH LABORATORY
ABERDEEN PROVING GROUND, MARYLAND

DTIC FILE COPY

85 9 03 013

**Destroy this report when it is no longer needed.
Do not return it to the originator.**

**Additional copies of this report may be obtained
from the National Technical Information Service,
U. S. Department of Commerce, Springfield, Virginia
22161.**

**The findings in this report are not to be construed as an official
Department of the Army position, unless so designated by other
authorized documents.**

**The use of trade names or manufacturers' names in this report
does not constitute indorsement of any commercial product.**

UNCLASSIFIED

SECURITY CLASSIFICATION OF THIS PAGE (When Data Entered)

REPORT DOCUMENTATION PAGE		READ INSTRUCTIONS BEFORE COMPLETING FORM
1. REPORT NUMBER MEMORANDUM REPORT BRL-MR-3451	2. GOVT ACCESSION NO. AD-A159324	3. RECIPIENT'S CATALOG NUMBER
4. TITLE (and Subtitle) WAVE MOTION ANALYSIS OF A NON-SPINNING LIQUID FILLED CYLINDER	5. TYPE OF REPORT & PERIOD COVERED Final	
7. AUTHOR(s) Paul Weinacht and Charles J. Nietubicz	6. CONTRACT OR GRANT NUMBER(s)	
9. PERFORMING ORGANIZATION NAME AND ADDRESS U.S. Army Ballistic Research Laboratory ATTN: AMXBR-LFD Aberdeen Proving Ground, Maryland 21005-5066	10. PROGRAM ELEMENT, PROJECT, TASK AREA & WORK UNIT NUMBERS RDT&E 1L162622A554	
11. CONTROLLING OFFICE NAME AND ADDRESS US Army Ballistic Research Laboratory ATTN: AMXBR-OD-ST Aberdeen Proving Ground, Maryland 21005-5066	12. REPORT DATE June 1985	
14. MONITORING AGENCY NAME & ADDRESS (if different from Controlling Office)	13. NUMBER OF PAGES 48	
	15. SECURITY CLASS. (of this report) Unclassified	
	16a. DECLASSIFICATION/DOWNGRADING SCHEDULE	
16. DISTRIBUTION STATEMENT (of this Report) Approved for public release, distribution unlimited.		
17. DISTRIBUTION STATEMENT (of the abstract entered in Block 20, if different from Report)		
18. SUPPLEMENTARY NOTES This report supersedes IMR No. 812 dated April 1984.		
19. KEY WORDS (Continue on reverse side if necessary and identify by block number) Liquid Filled Shell Compressible Liquids Wave Motion Analysis Fluid Mechanics		
20. ABSTRACT (Continue on reverse side if necessary and identify by block number) The results of a wave motion analysis of a partially liquid-filled, non-spinning cylinder are described. The analysis was undertaken to determine the internal fluid motion of a partially liquid-filled shell when subjected to large impulsive pressures. The high pressure levels are formed from the rupture of an internal burster tube. The primary concern is the determination of the endwall and side wall pressure levels after the burster tube rupture. The final objective of this program is to develop a predictive capability which can be used for		

UNCLASSIFIED

SECURITY CLASSIFICATION OF THIS PAGE(When Data Entered)

20. ABSTRACT (Continued)

determining the effects of various liquids, ullages and burster pressure levels. This report describes an initial analysis of the fluid motion inside a partially liquid-filled, non-spinning cylinder subject to a large impulsive pressure at one end. The analysis presented, tracks the pressure wave motion as a function of time and uses conservation of mass and momentum principles to determine the fluid properties in front of and behind the pressure waves. The results show the effect of initial pressure level and ullage on the resulting end wall and side wall pressures as a function of time. The peak end wall pressure is found to vary directly with the initial pressure level. The time duration of the maximum pressure acting on the end wall is a strong function of the ullage and to a lesser degree on the bulk modulus of the liquid.

Applicable figures; Wave motion analysis, Fluid mechanics.

UNCLASSIFIED

SECURITY CLASSIFICATION OF THIS PAGE(When Data Entered)

TABLE OF CONTENTS

	<u>Page</u>
LIST OF ILLUSTRATIONS.....	5
I. INTRODUCTION.....	7
II. GOVERNING EQUATIONS.....	7
III. WAVE MOTION ANALYSIS.....	8
Fluid Motion as a Function of Time.....	9
1. Fluid Motion Before Fluid Interface Hits Endwall.....	9
2. Fluid Motion After Fluid Interface Hits Endwall.....	10
IV. RESULTS.....	11
A. Pressure Time-Space Diagram.....	11
B. Pressure on the Cylinder Endwall.....	12
C. Dimensional Results for a Typical Case.....	13
V. CONCLUSIONS.....	13
LIST OF SYMBOLS.....	45
DISTRIBUTION LIST.....	47

Accession For	
NTIS GRA&I <input checked="" type="checkbox"/> FERIC TAB <input type="checkbox"/> Unannounced <input type="checkbox"/> Classification _____	
B. Distribution/ Availability Codes _____ Avail and/or Dist Special	
A1	



LIST OF ILLUSTRATIONS

<u>Figure</u>		<u>Page</u>
1	Setup for Idealized Problem.....	15
2	Control Volume for Solution of Mass and Momentum Equations.....	16
3	Propagation of Initial Pressure Wave.....	17
4	Reflection of Initial Pressure Wave from Liquid Interface.....	18
5	Reflection of Initial Pressure Wave from Pressurized Surface....	19
6	Generation of Secondary Pressure Wave by Collision of Interface with the Endwall.....	20
7	Reflection of Primary Pressure Wave from Pressurized Surface....	21
8	First Crossing of Primary and Secondary Pressure Waves.....	22
9	Reflection of Primary and Secondary Wave from Upper and Lower Surfaces.....	23
10	Second Crossing of Primary and Secondary Pressure Waves.....	24
11	Reflection of Primary and Secondary Waves from Lower and Upper Surfaces.....	25
12	Wave Status When Interface Impacts on Endwall.....	26
13	Pressure Time-Space Diagram, Fill Ratio = .97, Po/E = .035.....	27
14	Pressure Time-Space Diagram, Fill Ratio = .95, Po/E = .035.....	28
15	Pressure Time-Space Diagram, Fill Ratio = .93, Po/E = .035.....	29
16	Pressure Time-Space Diagram, Fill Ratio = .90, Po/E = .035.....	30
17	Pressure Time-Space Diagram, Fill Ratio = .95, Po/E = .025.....	31
18	Pressure Time-Space Diagram, Fill Ratio = .95, Po/E = .035.....	32
19	Pressure Time-Space Diagram, Fill Ratio = .95, Po/E = .05.....	33
20	Pressure Time-Space Diagram, Fill Ratio = .95, Po/E = .10.....	34
21	Endwall Pressure versus Time, Fill Ratio = .97, Po/E = .035.....	35
22	Endwall Pressure versus Time, Fill Ratio = .95, Po/E = .035.....	36
23	Endwall Pressure versus Time, Fill Ratio = .93, Po/E = .035.....	37
24	Endwall Pressure versus Time, Fill Ratio = .90, Po/E = .035.....	38



LIST OF ILLUSTRATIONS (Cont'd)

<u>Figure</u>		<u>Page</u>
25	Endwall Pressure versus Time, Fill Ratio = .95, Po/E = .025.....	39
26	Endwall Pressure versus Time, Fill Ratio = .95, Po/E = .035.....	40
27	Endwall Pressure versus Time, Fill Ratio = .95, Po/E = .05.....	41
28	Endwall Pressure versus Time, Fill Ratio = .95, Po/E = .10.....	42
29	Endwall Pressure versus Time, Dimensional Result.....	43

I. INTRODUCTION

The forced liquid project is being directed by the Munitions Branch of CRDC. The present task is to determine the internal reaction of a partially, liquid-filled shell subjected to large impulsive pressures from burster tube rupture. The main area of concern is the determination of the end wall and side wall pressures due to the sudden application of pressure at one end. A final objective is the development of a predictive capability which can be used to analyze the internal flow and quantify the internal pressure levels based on various liquids, ullages, and initial pressures.

II. GOVERNING EQUATIONS

The prediction of the fluid motion within a liquid-filled shell after a burster tube breaks is complicated by such factors as non-uniform geometry inside the shell, burster fragments, gas-liquid interaction, and release of pressure from the burster tube which may not remain at a constant level over the duration of the event. However, much of the basic physics which occurs inside the shell may be highlighted by examining the following highly simplified problem.

A cylindrical container of length, H , is filled with a fluid to a height L . The fluid is characterized by a density, ρ , and a bulk modulus, E . The portion of the container not occupied by fluid, the ullage, is assumed to be vacuum. Initiation of the event occurs with the application of a pressure step of magnitude, P_0 , applied to the lower surface of the fluid (see Figure 1). This pressure step generates a compression wave which propagates up the fluid slug. The ensuing fluid motion, which is assumed to occur isothermally, may be predicted by applying the equations of mass and momentum conservation across the pressure wave. A control volume, such as that shown in Figure 2, is fixed to move with the pressure wave at the speed of sound, c . Denoting the properties in front of the wave by the subscript 1 and properties behind the wave by 2, the mass and momentum equations are written below in terms of the pressure, P , density, ρ , fluid velocity, V , and wave speed, c .

Continuity

$$\rho_1 c = \rho_2 (c + V_1 - V_2) \quad (1)$$

Momentum

$$P_1 - P_2 = c^2 \rho_1 - (c + V_1 - V_2)^2 \rho_2 \quad (2)$$

An equation of state of the fluid is also required for the solution of these equations. In this analysis a simple equation of state is used.

$$\frac{\partial P}{\partial \rho} = E/\rho \quad (3)$$

Since the properties in front of the wave are known, one additional equation is required in order to solve for the four unknowns of interest; the wave speed, and the fluid pressure, density, and velocity behind the wave. This additional equation is, in a sense, a boundary condition, and is dependent on the manner in which pressure waves are generated or reflected at the fluid boundaries.

For a wave generated by a change in pressure at a boundary, the pressure behind the wave will be equal to the new pressure level. The boundary condition for a wave reflecting from a surface will depend on whether the surface is "free" or constrained. The pressure behind a wave reflecting from a free surface will be equal to the pressure outside the free surface, while the velocity behind a wave reflecting from a constrained surface (such as the end-wall) will be zero. The velocity behind a wave generated by the collision of a free surface with a constrained surface is also zero. These conditions are expressed below.

For a wave generated by a change in pressure at a boundary, or wave reflected from a free surface,

$$P_2 = P_{\text{BOUNDARY}} . \quad (4a)$$

For a wave reflected from a constrained surface, or a wave generated by collision of a free surface with a constrained surface,

$$V_2 = 0 . \quad (4b)$$

In the case of two pressure waves crossing each other, continuity and momentum equations are applied across each wave and are solved simultaneously for the conditions between the two waves.

In this analysis, the pressure waves generated are assumed to be weak; thus the velocity of the fluid is small compared to the speed of sound and the changes in density of the fluid are small compared with the initial fluid density. Thus, the wave speed may be expressed as follows;

$$c = \sqrt{E/\rho} . \quad (5)$$

III. WAVE MOTION ANALYSIS

Using the equations described above, the motion of the fluid as a function of time has been determined. In this section a description of the predicted fluid motion is given.

Fluid Motion as a Function of Time

The pressure step, which is applied to the lower surface of the fluid, generates a compression wave which begins to accelerate the fluid toward the cylinder endwall. After the fluid interface strikes the endwall, an additional pressure wave begins propagating throughout the fluid. Thus, a description of the fluid motion involves the tracking of these two pressure waves as they move throughout the fluid slug. It is useful, then, to separate the motion into two phases; the motion of the fluid before the collision of the free surface with the endwall, involving a single pressure wave, and the motion after the interface impacts on the endwall, involving the motion of two waves.

1. Fluid Motion Before Fluid Interface Hits Endwall

The application of the pressure step to the lower surface of the fluid generates a compression wave which propagates up the fluid slug at the speed of sound of the liquid, c . As shown in Figure 3, the fluid is motionless and at vacuum in front of pressure wave, while behind the wave the fluid is at pressure P_0 and moving upwards with velocity, V_0 . (In Figures 3-11, compression and expansion waves are denoted by filled and unfilled arrows, respectively. The direction of the propagation of each wave is shown by the arrow.) The ratio of fluid velocity behind this wave, V_0 , to the speed of sound, determined by application of the above equations, is approximately equal to the ratio of P_0 to the liquid bulk modulus.

$$V_0/c \approx P_0/E$$

Typically then, V_0 will be three to ten percent of the speed of sound for this problem.

This compression wave will propagate up the fluid slug until it reaches the upper fluid surface, at which time it will reflect as an expansion wave traveling down the fluid at the speed of sound (Figure 4). Behind the expansion wave the fluid is moving upwards at velocity $2V_0$ and is at zero pressure. The expansion wave will propagate down the fluid until reaching the lower pressurized surface, reflecting as a compression wave, behind which the fluid will be moving upwards at velocity $3V_0$ (Figure 5). This wave will continue to propagate up and down the fluid slug with the velocity behind the wave increasing by V_0 each time the pressure wave reflects from the upper or lower surface of the fluid.

At some time, however, the fluid interface, which begins moving after the initial arrival of the compression wave, will impact on the cylinder endwall, bringing the fluid locally to rest and generating an additional compression wave. The strength of this compression wave is dependent on the velocity of the fluid interface as it strikes the endwall, which increases by $2V_0$ each time the initial pressure wave reflects from the fluid interface. The velocity of the interface as it strikes the endwall will thus depend on the length of the cylinder, H , the length of the fluid slug, L , the speed of sound, c , the initial pressure, P_0 , and the bulk modulus, E . This relationship is shown nondimensionally in Figure 12 in terms of the fill ratio, which is the ratio of the length of the fluid slug to the length of the cylinder, and the ratio of initial pressure to bulk modulus.

Values of fill ratio and initial pressure to bulk modulus ratio which lie in region I represent cases where the initial pressure wave will reflect from the fluid interface only once before the interface impacts on the endwall. Thus, the velocity of the interface for these cases will be $2V_0$. Values of fill ratio and initial pressure to bulk modulus ratio which lie in Region II, represent cases where the initial pressure wave will reflect twice from the fluid interface before the interface impacts on the endwall, yielding a interface velocity on impact of $4V_0$. Points below region II represent cases where 3 or more reflections are expected. Typical fill ratios and initial pressure to bulk modulus ratios for the problem of interest lie in Region I; thus the examination of the fluid motion after the interface impacts on the endwall need only focus on the cases where the initial pressure wave reflects from the interface only once.

2. Fluid Motion After Fluid Interface Hits Endwall

For fill ratios and initial pressure to bulk modulus ratios of interest, then, the upper surface of the fluid will impact on the cylinder endwall after the arrival of the initial pressure wave, but before this pressure wave reflects from the lower surface of the fluid and returns. The collision of the fluid interface with the cylinder endwall will generate a secondary compression wave which travels down the fluid slug. Behind the secondary wave the fluid is brought to rest, doubling the pressure. The state of the fluid motion at this point in time is shown in Figure 6. (The primary wave is shown as a solid line, while the secondary wave is shown as a dashed line.) Both pressure waves move down the fluid slug until the primary wave reaches the pressurized surface and reflects as a compression wave, as shown in Figure 7. Behind this compression wave the fluid velocity is increased to $3V_0$.

The crossing of the primary and secondary pressure waves, shown in Figure 8, causes the pressure between the two waves to increase to $3P_0$ and the velocity to decrease to V_0 .

The primary wave continues moving up and reflects as a compression wave after reaching the endwall. Between this compression wave and the endwall the pressure is increased to $4P_0$. The secondary pressure wave moves toward the pressurized surface and reflects as a expansion wave. The fluid behind this wave is now moving away from the endwall at velocity V_0 . The fluid is now at the state shown in Figure 9.

The two pressure waves again cross, dropping the pressure between them to $2P_0$ and causing the fluid between the two waves to move at $2V_0$ in the direction away from the endwall. This is shown in Figure 10.

The secondary pressure wave continues moving toward the endwall and reflects as an expansion wave, dropping the pressure between the endwall and the wave to vacuum. The primary wave also reaches the pressurized surface and reflects as an expansion wave, as shown in Figure 11. The pressure waves will continue to move throughout the fluid until they are damped out by viscous effects. (In this analysis there is no damping of the waves since viscous effects are neglected.) At this point the analysis is discontinued, because the maximum pressure at the endwall ($4P_0$) has been relieved.

IV. RESULTS

Results for the pressure as a function of space and time are presented in nondimensional form. Endwall pressure as a function of time, again nondimensionalized, is examined and compared with an existing theory. Finally, dimensional results are presented for a typical case to provide insight into the physical problem of interest.

A. Pressure Time-Space Diagram

With the fluid motion defined over the time interval of interest, a plot of the pressure as a function of time and space can be constructed for a given fill ratio and initial pressure to bulk modulus ratio. Figures 13-16 show the pressure time-space diagram for a constant pressure to bulk modulus ratio ($P_0/E = .035$) and for four different fill ratios of interest, .97, .95, .93, and .90. Figures 17-20 display the pressure time-space diagram for a single fill ratio (.95) and varying pressure to bulk modulus ratio, .025, .035, .05, and .10. Time has been nondimensionalized by the time required for a pressure wave to travel the length of the fluid slug. The vertical ordinate represents the axial position from the bottom cylinder nondimensionalized by the cylinder length. The pressure at a particular instant in time and at a particular axial position is represented by the shading at the appropriate location on the graph.

The position of the upper and lower fluid surfaces as a function of time are shown by the thickened lines on the upper and lower portions of the figures, while the position of the primary and secondary pressure waves are represented by the thin solid and dashed lines respectively.

These figures may be used to determine the pressure as a function of time at a particular axial position within the cylinder by drawing a horizontal line at the appropriate vertical ordinate on the graph. Similarly, the spacial distribution of pressure at a particular instant in time is represented by a vertical line at the appropriate horizontal ordinate.

Figure 13 displays the pressure history for what may be a typical case of interest; .97 fill ratio, P_0 of 241.0 MPa, and bulk modulus of 6895. MPa (water subject to a pressure of 689.5 MPa has a similar bulk modulus).¹ After the collision of the interface with the endwall, a region of pressure $2P_0$ is seen to develop. This region extends over a large portion of the cylinder, from the endwall to the lower 30% of the cylinder. Adjacent to the region of $2P_0$ are two regions of high pressure of magnitude $3P_0$ and $4P_0$. The region of $4P_0$ begins at the endwall after the collision of the primary wave with the endwall, and is seen to occur only in the top 25% of the cylinder. Nearly the entire length of the cylinder appears to experience a pressure of $3P_0$ over a small period of time for this case.

The effect of changing the fill ratio is shown in Figures 13-16. Decreasing the fill ratio is seen to increase the duration and extent of the

1. C. Carmichael, "Kent's Mechanical Engineers' Handbook," Design and Production, Twelfth Edition, Wiley Handbook Series, 1964.

region of pressure $4P_0$. At the fill ratio of 90% the region of $4P_0$ extends over the upper 60% of the cylinder and lasts nearly four times longer than the adjacent region of $2P_0$ at the endwall. Interestingly, the size of the region of pressure $3P_0$ seems to increase with decreasing fill ratio until it reaches a maximum value, and then seems to decrease.

The effect of changing the ratio of P_0 to the bulk modulus while holding the fill ratio constant is shown in Figures 17-20. These figures demonstrate the effect of changing the initial pressure P_0 and/or changing the bulk modulus of the fluid.

In the case of changing the initial pressure P_0 , the duration and extent of the $4P_0$ region is seen to decrease with increasing initial pressure. Thus, while the peak pressure on the endwall can be increased by increasing the initial pressure, the duration of this pressure will decrease somewhat.

Additionally, if the bulk modulus of the fluid is changed, this theory predicts that the duration of the peak pressure region will decrease as the bulk modulus is decreased (as the fluid is made more compressible), but the magnitude of the peak pressure will remain constant.

In Figures 13-20 the degree to which the fluid column is compressed is seen by comparing the initial length of the fluid column with the length at a later time. Compression of 10%-40% is seen and is reflective of the very high pressure levels which the fluid experiences.

B. Pressure on the Cylinder Endwall

The pressure on the endwall of the cylinder as a function of time is an item of significant interest in this project. These pressures, for the cases discussed above, have been taken from Figures 13-20 and replotted in Figures 21-28. Also displayed on these figures are the values determined by a previous theory.² In that analysis, the motion of the fluid slug was treated as a rigid body until it collided with the endwall. A pressure wave was then generated and traveled down the fluid slug. This resulted in a single pressure jump, to a maximum pressure which remained constant in time.

The endwall pressure, as predicted in the current analysis, is zero until the fluid interface collides with the endwall, increasing the pressure to $2P_0$ as the secondary pressure wave is generated. The arrival of the primary wave at a later time increases the pressure further to $4P_0$. The endwall pressure is later relieved to vacuum as the secondary pressure returns.

Figures 21-24 show that decreasing the fill ratio increases the duration of the peak pressure $4P_0$ substantially, while decreasing the duration of the $2P_0$ pressure level. In contrast to the previously proposed theory which predicts a single jump in the endwall pressure whose magnitude is a function of the fill ratio, the current analysis predicts, for the fill ratios of

2. J. L. Watson, B. P. Burns, and J. M. Bender, "An Analysis of a Previously Unexplained Event (U)," U.S. Army Ballistic Research Laboratory, Aberdeen Proving Ground, Maryland, ARBRL-MR-03227, November 1982 (CLASSIFIED).

interest, a maximum pressure level ($4P_0$) independent of fill ratio, but the duration which increases with decreasing fill ratio.

Figures 25-28 demonstrate the effect on the endwall pressure of changing the initial pressure to bulk modulus ratio. As was seen before, increasing the bulk modulus increases the duration over which the peak pressure of $4P_0$ acts. Increasing the initial pressure P_0 will increase the peak endwall pressure proportionately, while decreasing the duration somewhat.

Interestingly, averaging the endwall pressure predicted by the current theory over the time where the endwall pressure is $2P_0$ to $4P_0$ yields a value similar to that predicted by the previous theory. This is because the rigid body assumption of the previous theory treats the motion of the fluid slug in global or average sense, while the current theory treats the motion more discretely. Correspondingly, these results indicate that the more compressible the fluid, the greater the difference in the predicted peak pressures between the two theories.

C. Dimensional Results for a Typical Case

In order to gain a better feeling for the magnitude of the physical variables of interest, endwall pressure as a function of time is presented for the following case.

$$\begin{aligned} H &= .67 \text{ m} \\ E &= 6895 \text{ MPa} \\ P_0 &= 241 \text{ MPa} \\ \rho &= 1000 \text{ kg/m}^3 \\ \text{Fill ratio} &= .95 \end{aligned}$$

Since the ratio of the initial pressure to the liquid bulk modulus is .035 and the fill ratio is .95, the results for one of the cases obtained previously (Figure 26) may be applied. The dimensionalized result for endwall pressure as a function of time for this case is shown in Figure 29. As before, the pressure first jumps to twice the value (482 MPa) of the initial pressure step before jumping to the four times (964 MPa) the initial pressure value. The time over which the pressures $2P_0$ and $4P_0$ act are .3 and .17 milliseconds, respectively, and the entire process is completed in about 1. millisecond.

V. CONCLUSIONS

The results of this analysis provide significant insight into the physical processes which may occur in a liquid-filled shell subject to large initial pressures, and stress the importance of modeling the compressibility of the fluid within the shell for the current problem of interest.

The motion of the fluid is driven by two pressure waves, one generated by the initial pressure step and another generated by the collision of the fluid with the endwall. The highest pressure levels occur for a longer duration near the top of the cylinder. The theory predicts that decreasing the fill ratio will increase the duration of the peak pressure at the endwall but not

the magnitude for the range of fill ratios and initial pressure to bulk modulus ratios currently of interest. This peak pressure will be four times the value of the initial pressure step. The analysis indicates that peak pressures greater than four times the initial pressure step are possible for fill ratios less than the values currently of interest. Increasing the magnitude of the initial pressure step will increase peak pressure proportionately, but the duration over which this peak pressure acts will be decrease slightly. Decreasing the bulk modulus of the fluid (i.e. making the fluid more compressible) will cause the duration of peak pressure to increase slightly.

It is acknowledged that this analysis does not model such effects as area change within the shell, changes in bulk modulus with pressure, and variation in the pressure at the lower surface of the fluid with time. The modeling of these effects is probably more suitably handled by numerical techniques. As this analysis has demonstrated, the numerical technique chosen should model the compressible nature of the fluid and have the capability to track moving pressure waves.

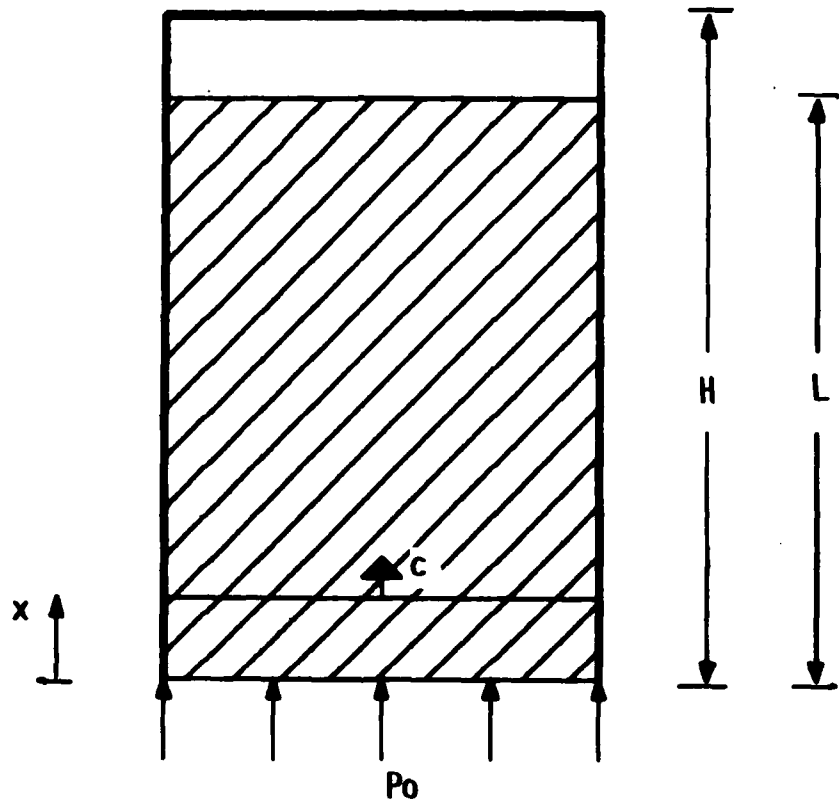


Figure 1. Setup for Idealized Problem

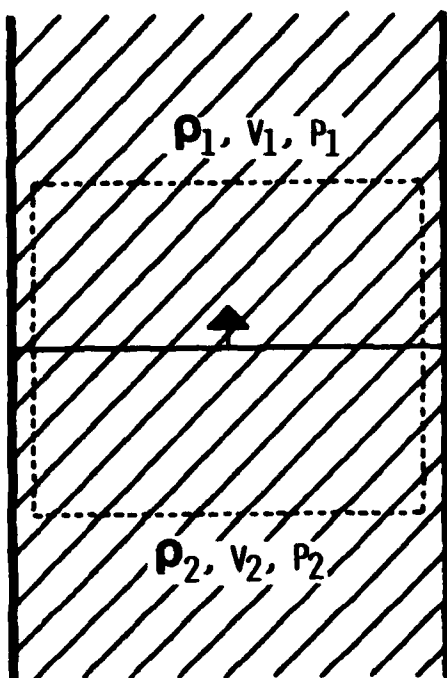


Figure 2. Control Volume for Solution of Mass and Momentum Equations

PRESSURE STEP IS APPLIED TO FLUID.
PRIMARY PRESSURE WAVE PROPAGATES
UP THE FLUID SLAB.

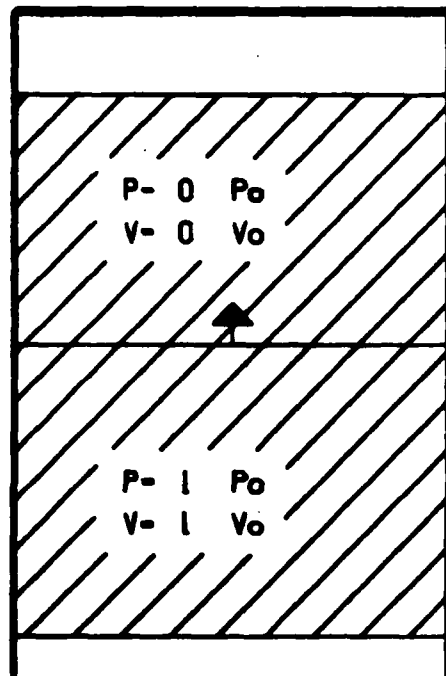


Figure 3. Propagation of Initial Pressure Wave

PRIMARY PRESSURE WAVE REACHES FLUID
INTERFACE AND RETURNS AS AN
EXPANSION WAVE.
INTERFACE BEGINS TO MOVE TOWARD
ENDWALL.

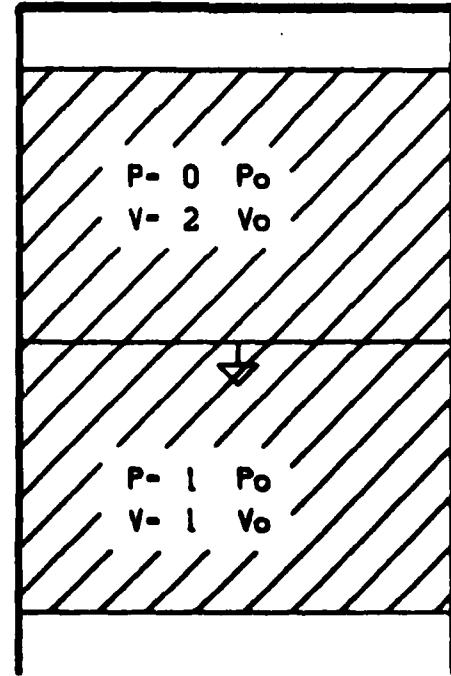


Figure 4. Reflection of Initial Pressure Wave from Liquid Interface

PRIMARY PRESSURE WAVE REACHES
PRESSURIZED SURFACE AND REFLECTS
AS A COMPRESSION WAVE.

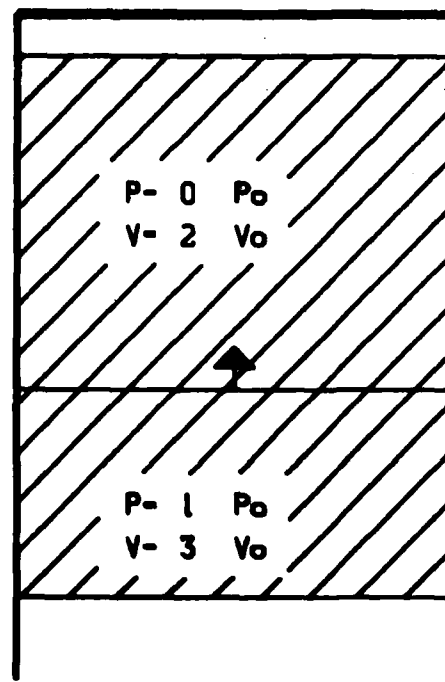


Figure 5. Reflection of Initial Pressure Wave from Pressurized Surface

FLUID INTERFACE COLLIDES WITH ENDWALL
AND GENERATES A SECONDARY COMPRESSION
WAVE THAT TRAVELS DOWN FLUID SLUB.

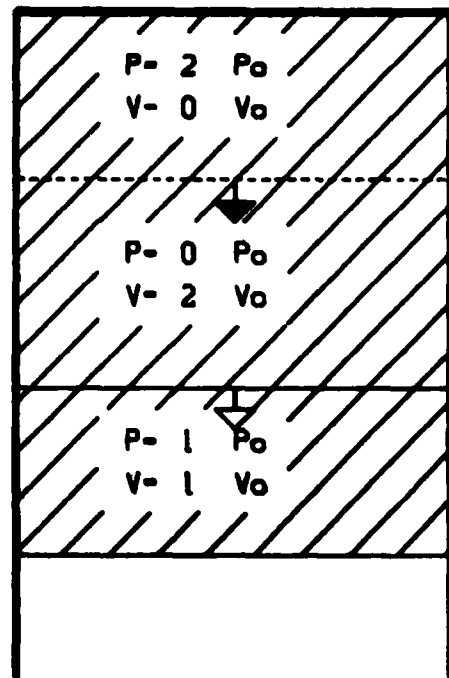


Figure 6. Generation of Secondary Pressure Wave by Collision of Interface with the Endwall

EXPANSION WAVE REACHES PRESSURIZED
SURFACE AND BEGINS MOVING TOWARD
ENDWALL AS A COMPRESSION WAVE.

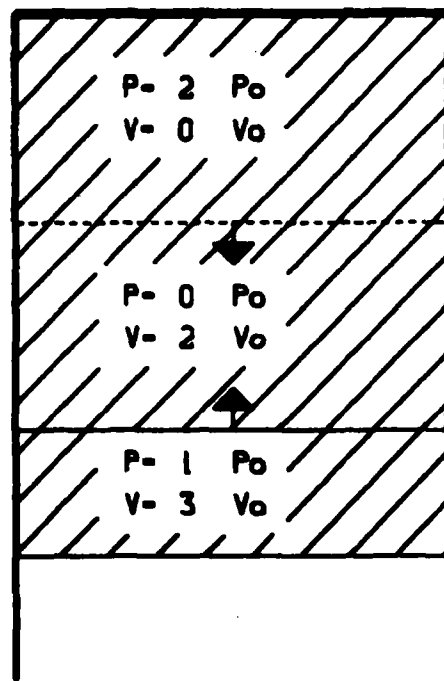


Figure 7. Reflection of Primary Pressure Wave from Pressurized Surface

PRIMARY AND SECONDARY COMPRESSION
WAVES CROSS.

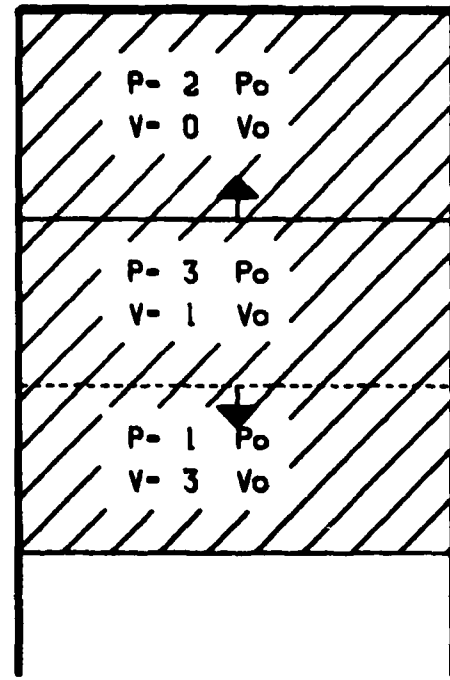


Figure 8. First Crossing of Primary and Secondary Pressure Waves

PRIMARY COMPRESSION WAVE REACHES
ENDWALL AND REFLECTS AS A COMPRESSION
WAVE. MAXIMUM PRESSURE OBTAINED ON
ENDWALL. SECONDARY COMPRESSION WAVE
REACHES PRESSURIZED SURFACE AND
REFLECTS AS AN EXPANSION WAVE.

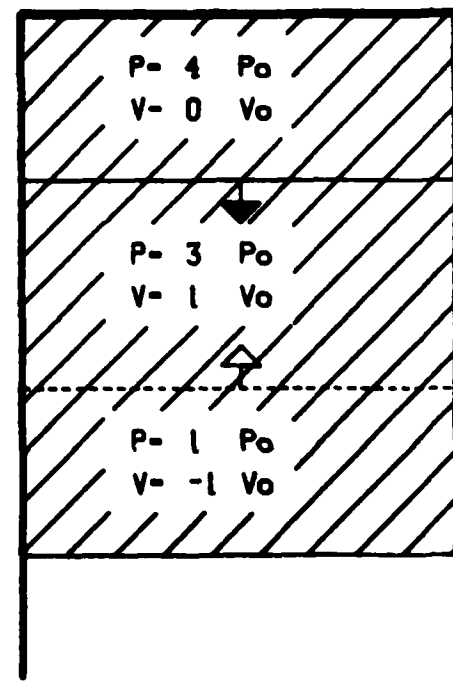


Figure 9. Reflection of Primary and Secondary Wave
from Upper and Lower Surfaces

PRIMARY COMPRESSION WAVE AND SECONDARY EXPANSION WAVE CROSS.

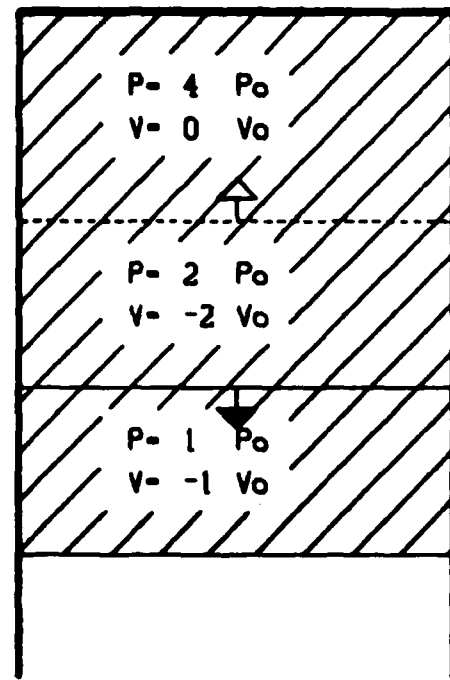


Figure 10. Second Crossing of Primary and Secondary Pressure Waves

PRIMARY WAVE REACHES PRESSURIZED
SURFACE AND RETURNS AS AN EXPANSION.
HIGH PRESSURE ON ENDWALL RELIEVED.
SECONDARY EXPANSION WAVE REACHES
ENDWALL AND REFLECTS AS AN EXPANSION
WAVE.

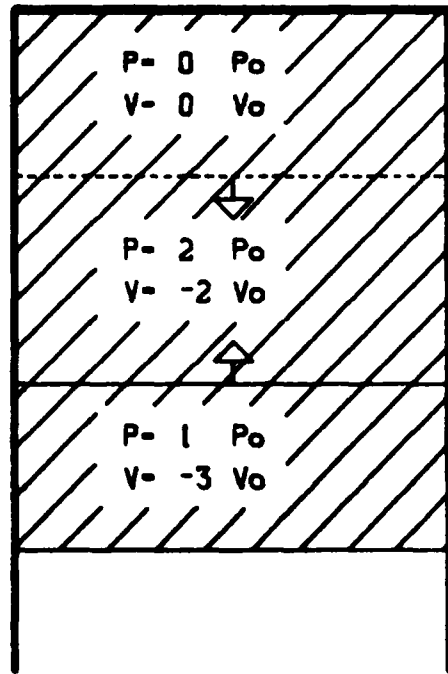


Figure 11. Reflection of Primary and Secondary Waves
from Lower and Upper Surfaces

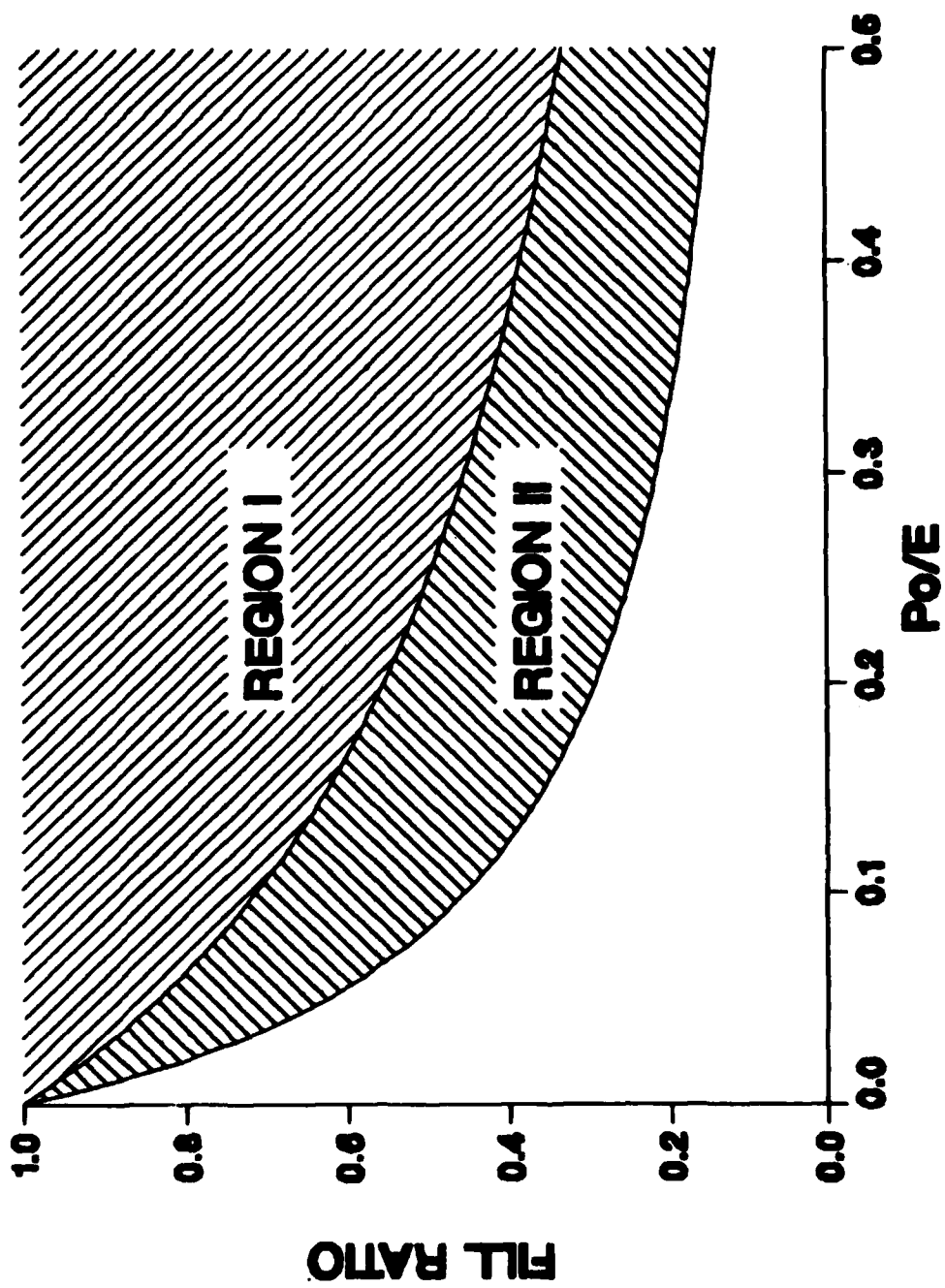


Figure 12. Wave Status When Interface Impacts on Endwall 11

PRESSURE TIME-SPACE DIAGRAM

FILL RATIO = 0.970 $P_0 / E = 0.035$

- $\square \quad 0$
- $\square \diagup P_0$
- $\square \diagdown 2P_0$
- $\square \times 3P_0$
- $\square \blacksquare 4P_0$

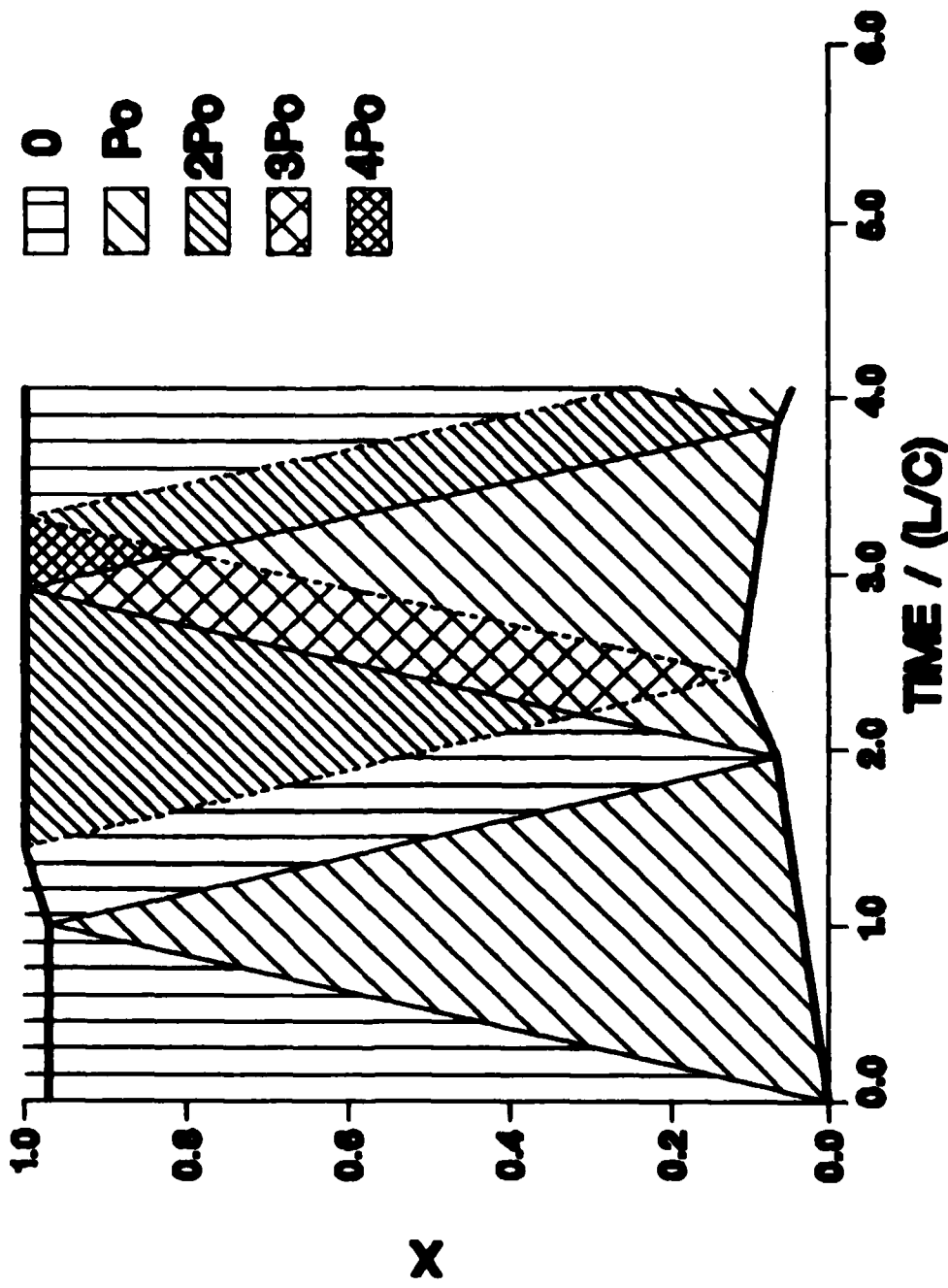


Figure 13. Pressure Time-Space Diagram, Fill Ratio = .97, $P_0/E = .035$

PRESSURE TIME-SPACE DIAGRAM

FILL RATIO = 0.950 $P_0 / E = 0.035$

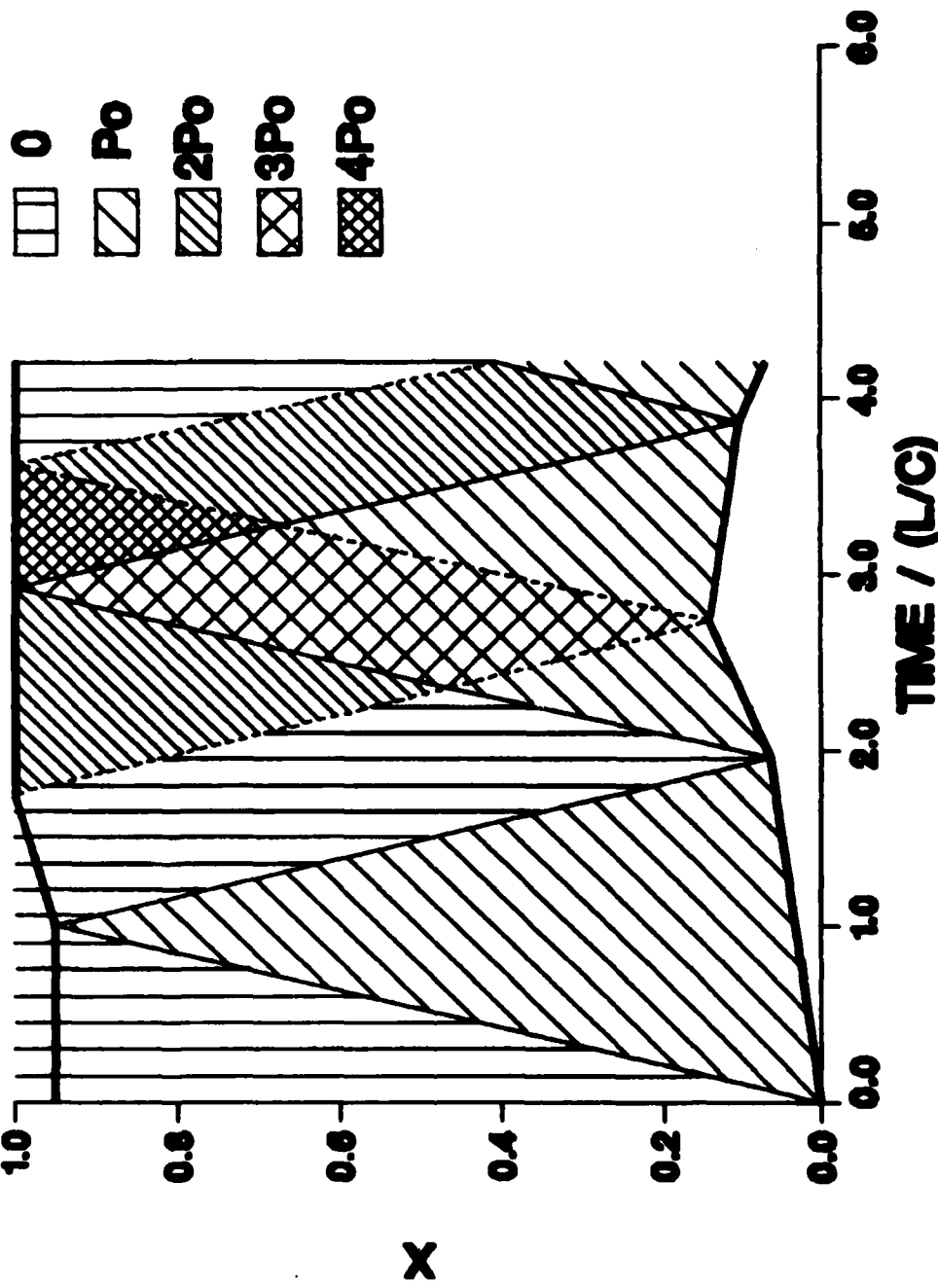


Figure 14. Pressure Time-Space Diagram, Fill Ratio = .95, $P_0/E = .035$

PRESSURE TIME-SPACE DIAGRAM

FILL RATIO = 0.930 $P_o / E = 0.035$

- $\square \square 0$
- $\square \backslash P_o$
- $\square \diagup 2P_o$
- $\square \times 3P_o$
- $\square \# 4P_o$

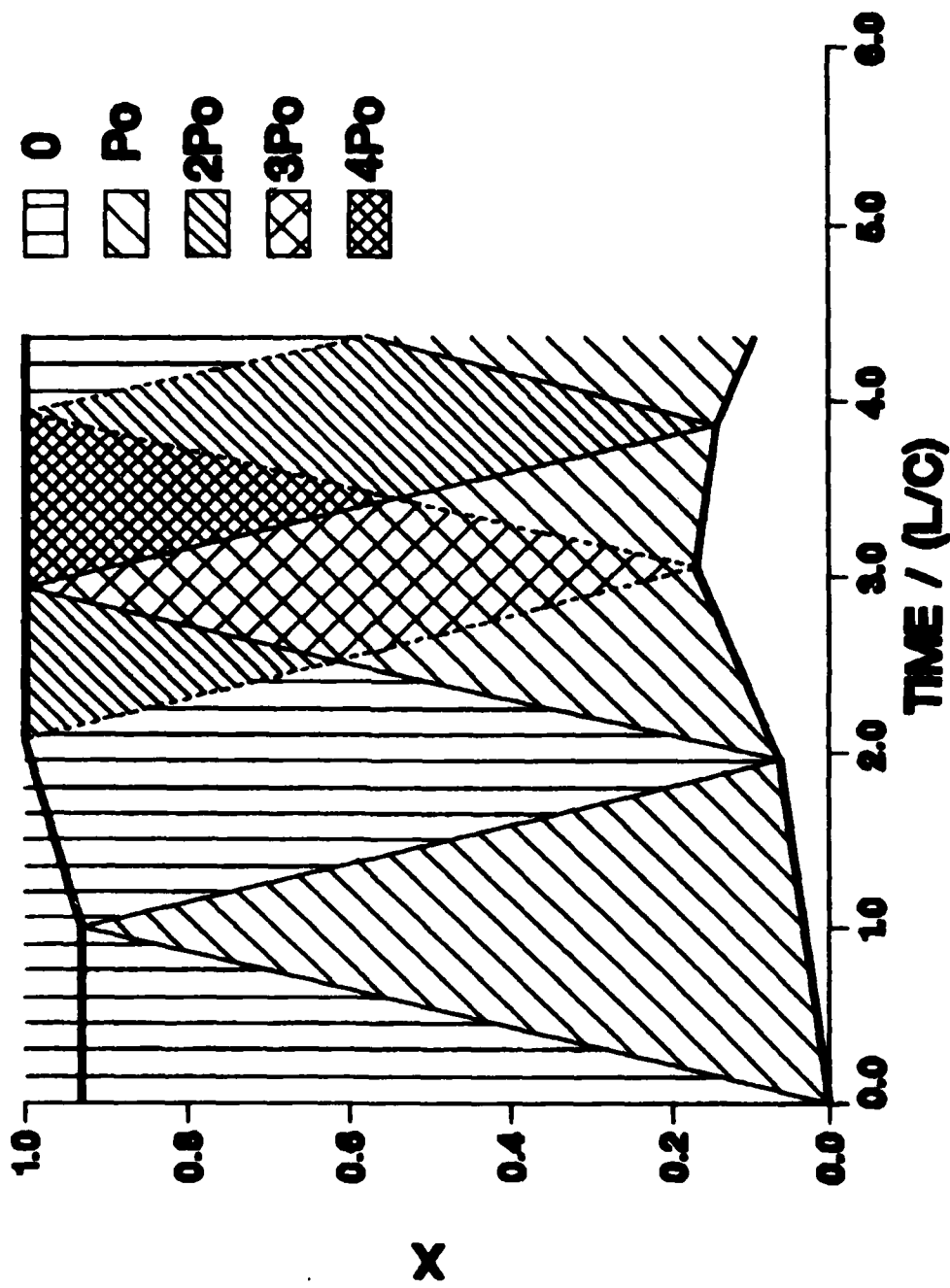


Figure 15. Pressure Time-Space Diagram, Fill Ratio = .93, $P_o/E = .035$

PRESSURE TIME-SPACE DIAGRAM

FILL RATIO = 0.900 $P_o / E = 0.035$

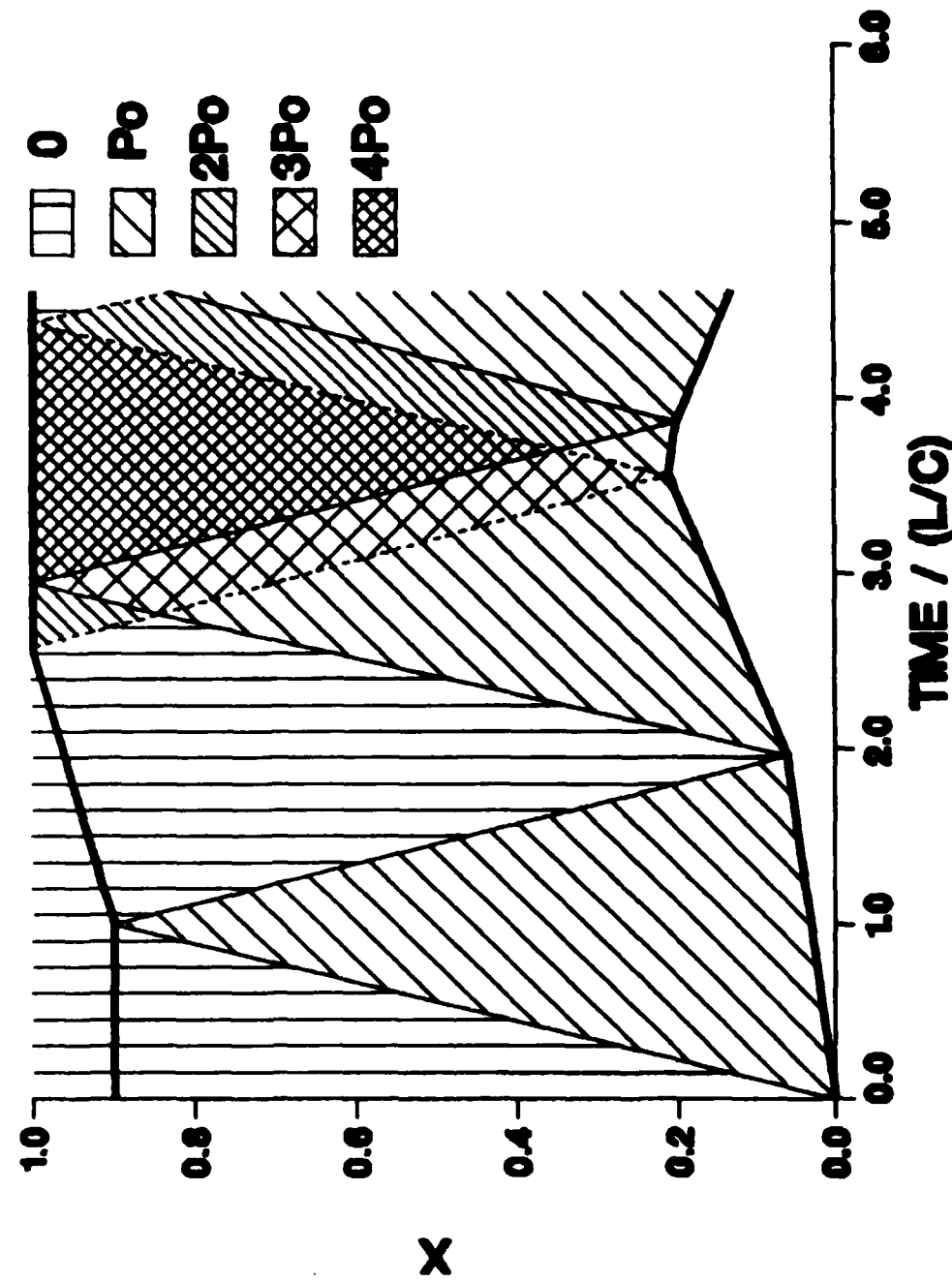


Figure 16. Pressure Time-Space Diagram, Fill Ratio = .90, $P_o/E = .035$

PRESSURE TIME-SPACE DIAGRAM

FILL RATIO = 0.950 $P_0 / E = 0.025$

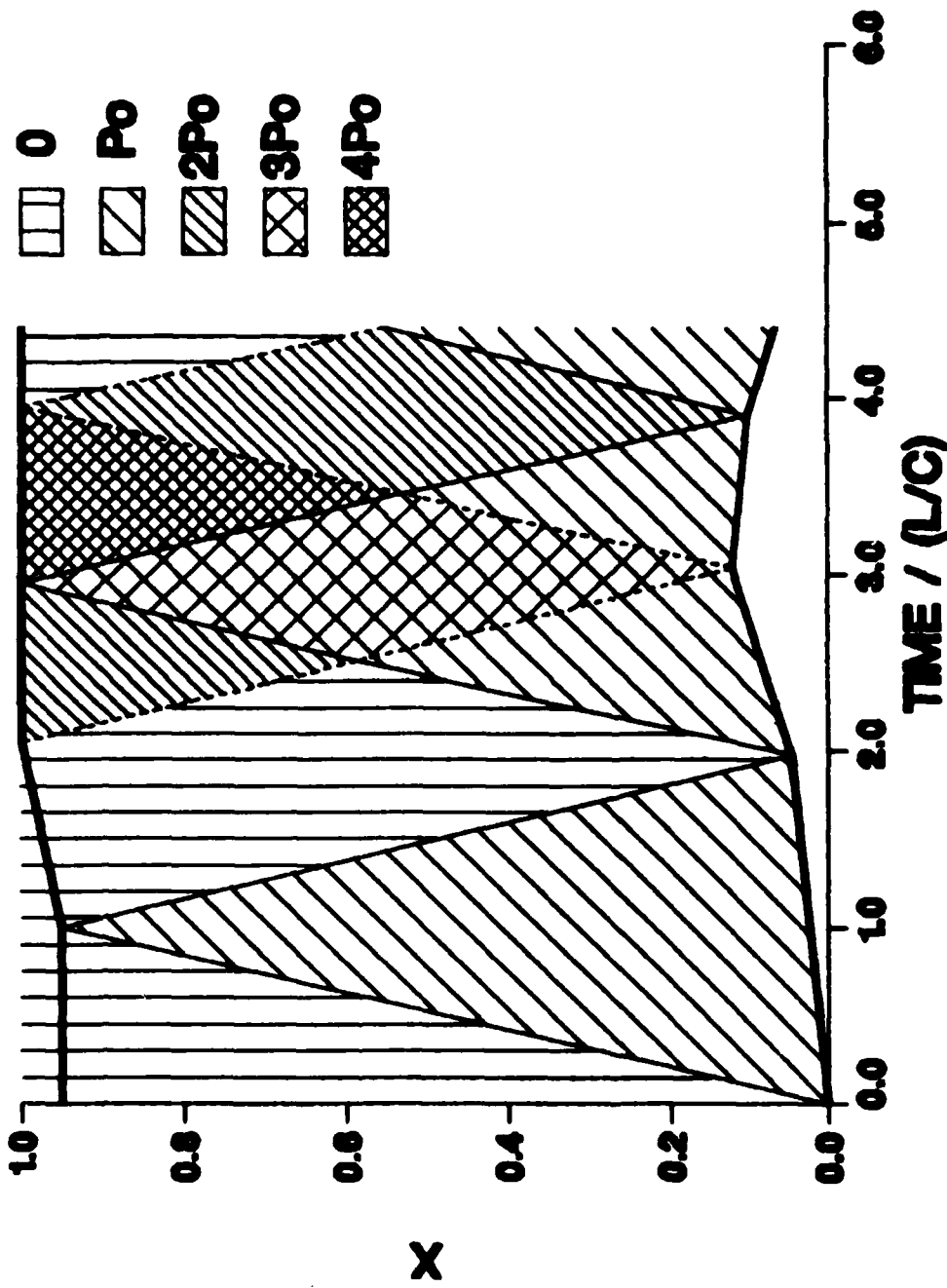


Figure 17. Pressure Time-Space Diagram, Fill Ratio = .95, $P_0/E = .025$

PRESSURE TIME-SPACE DIAGRAM

FILL RATIO = 0.950 $P_o / E = 0.035$

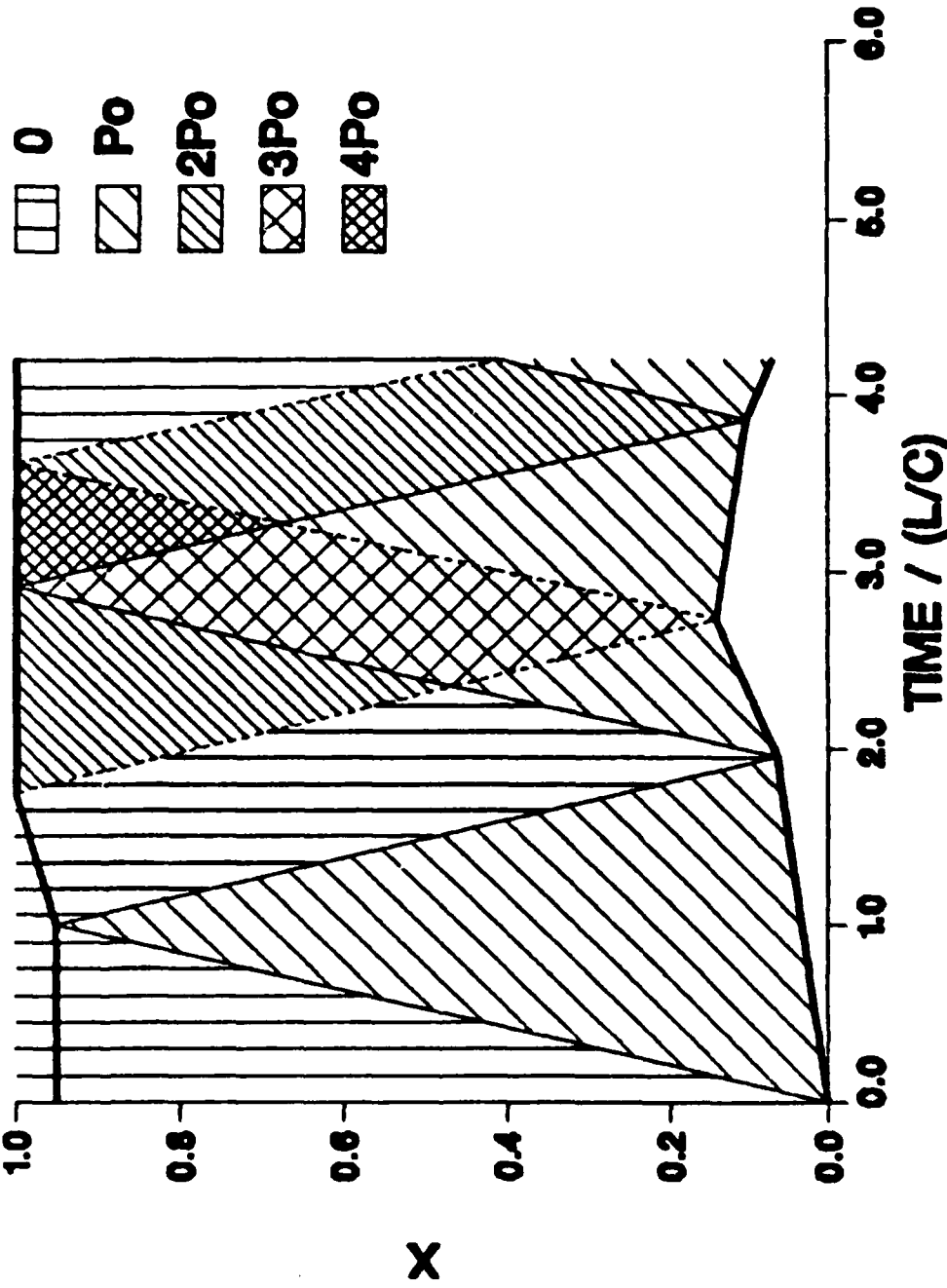


Figure 18. Pressure Time-Space Diagram, Fill Ratio = .95, $P_o/E = .035$

PRESSURE TIME-SPACE DIAGRAM

FILL RATIO = 0.950 $P_0 / E = 0.050$

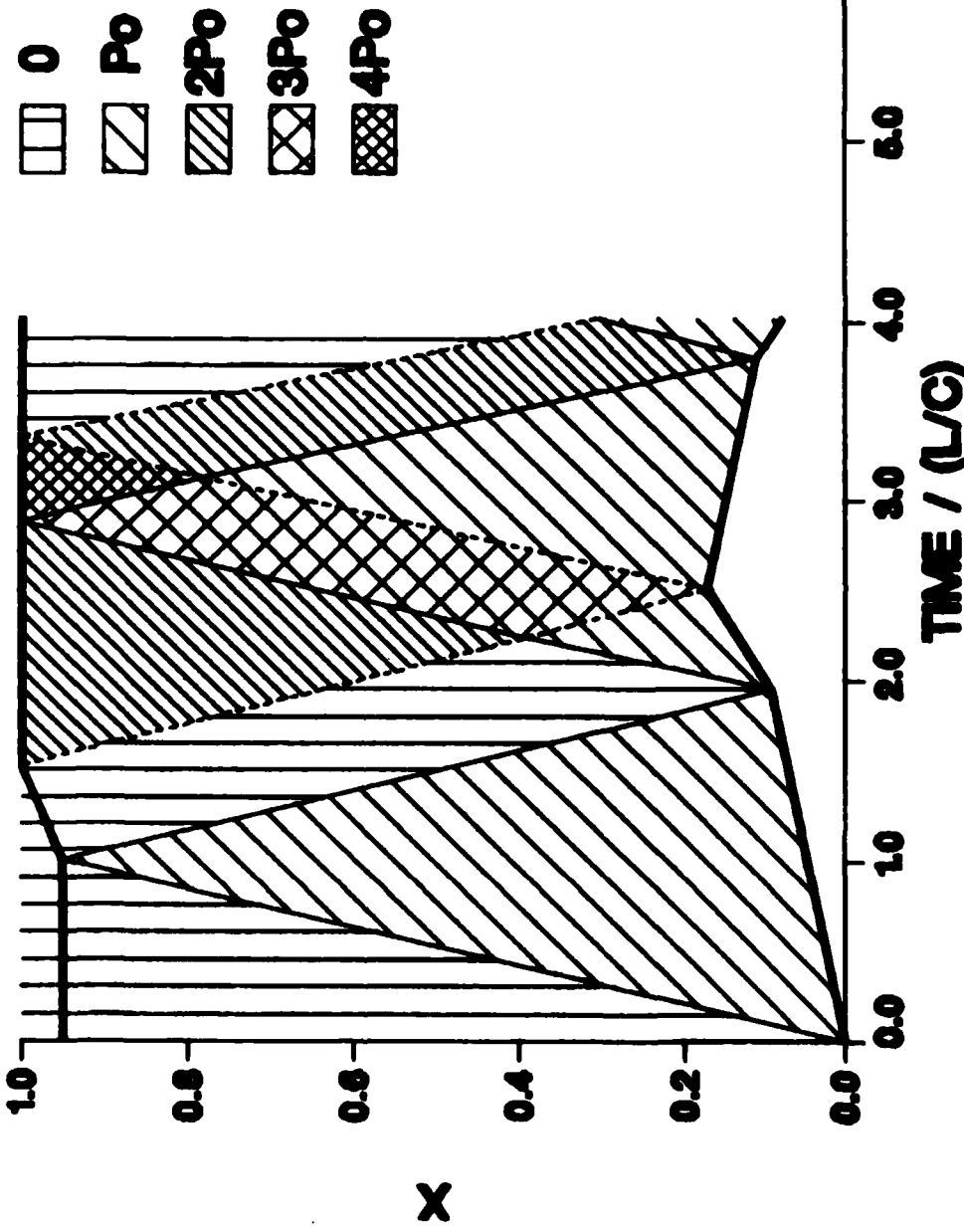


Figure 19. Pressure Time-Space Diagram, Fill Ratio = .95, $P_0/E = .05$

PRESSURE TIME-SPACE DIAGRAM

FILL RATIO = 0.950 $P_0 / E = 0.100$

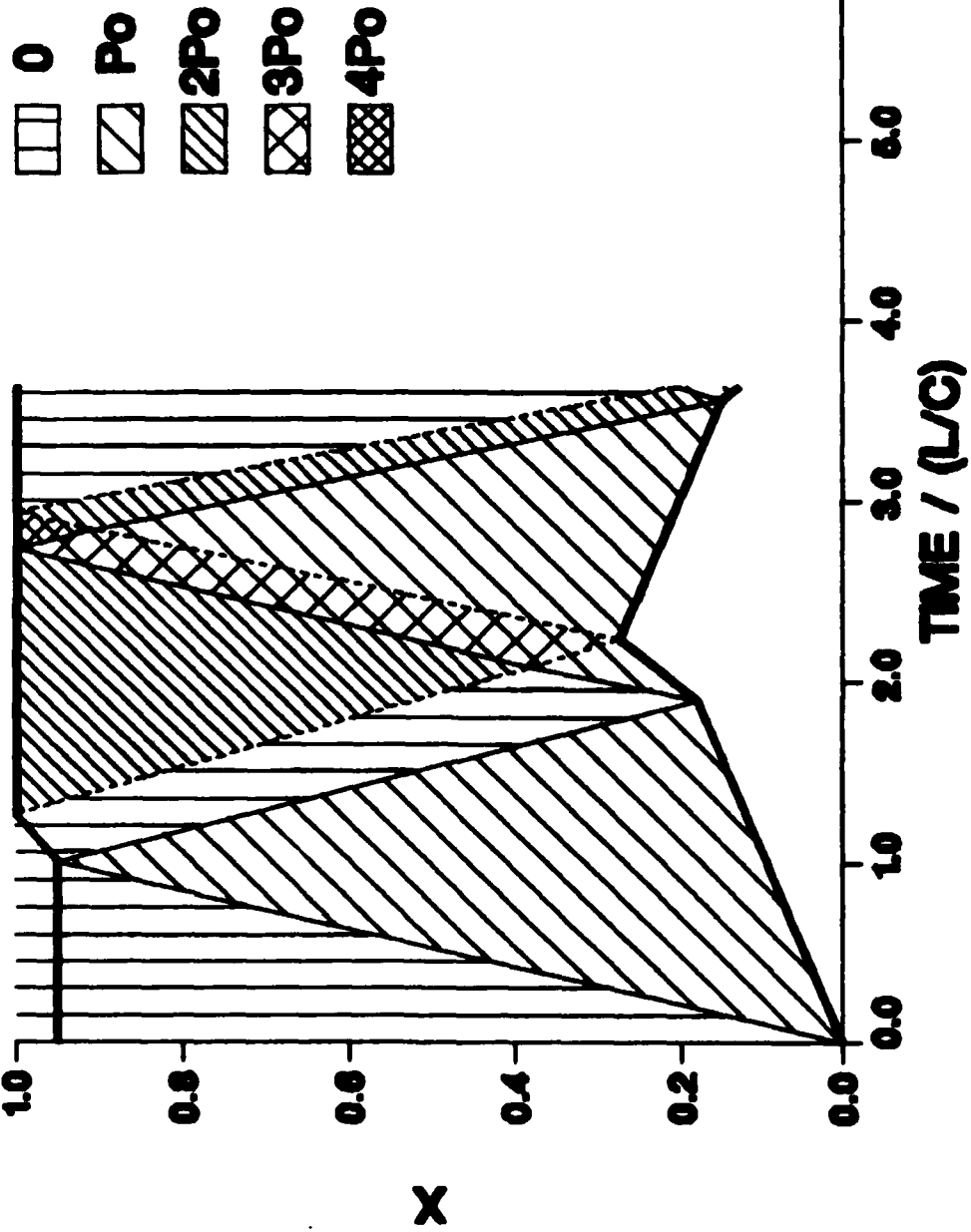


Figure 20. Pressure Time-Space Diagram, Fill Ratio = .95, $P_0/E = .10$

ENDWALL PRESSURE VERSUS TIME

$$\text{FILL RATIO} = 0.970 \quad P_0 / E = 0.035$$

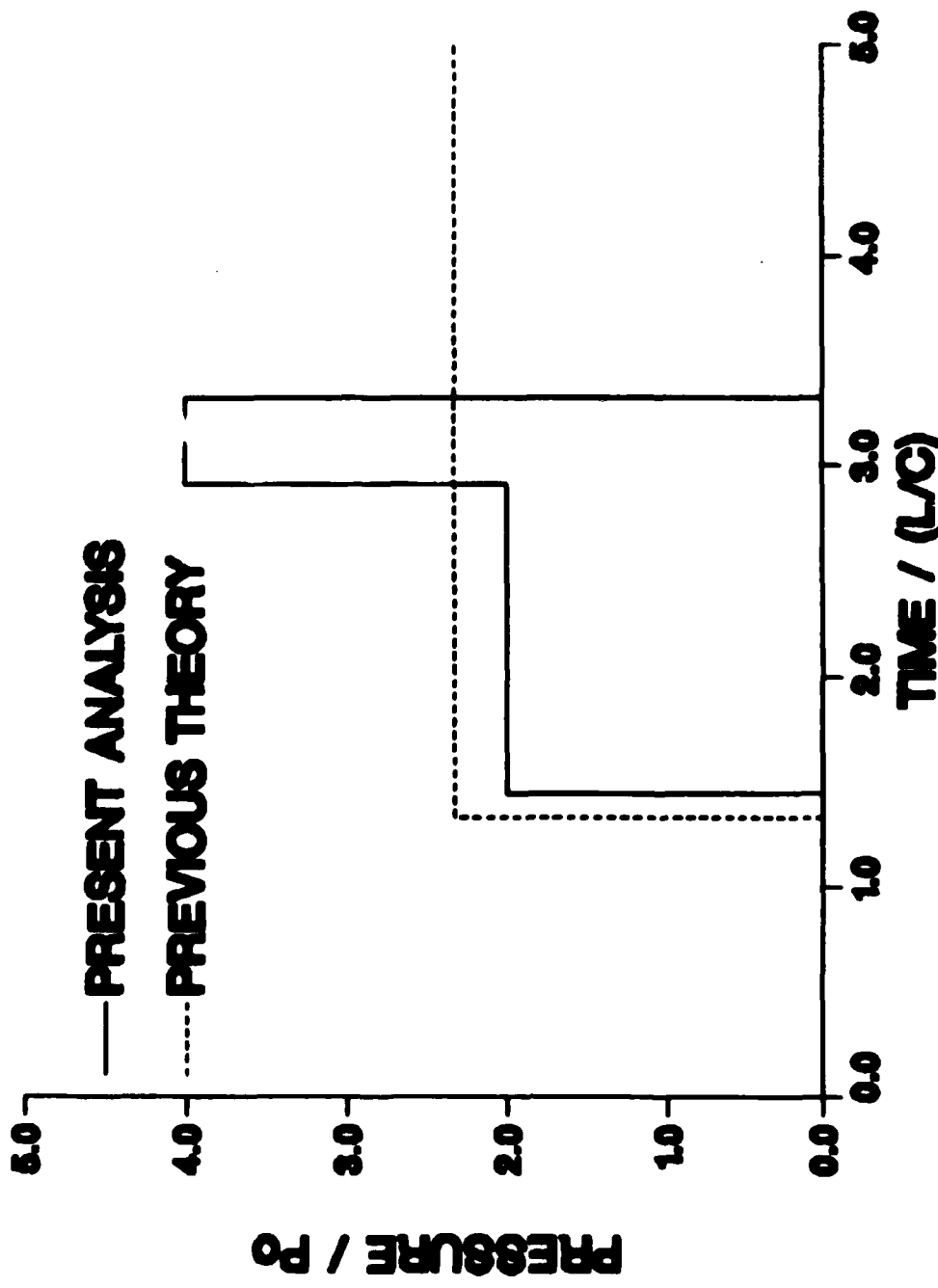


Figure 21. Endwall Pressure versus Time, Fill Ratio = .97, $P_0/E = .035$

ENDWALL PRESSURE VERSUS TIME

FILL RATIO = 0.950 $P_0 / E = 0.035$

— PRESENT ANALYSIS
- - - PREVIOUS THEORY

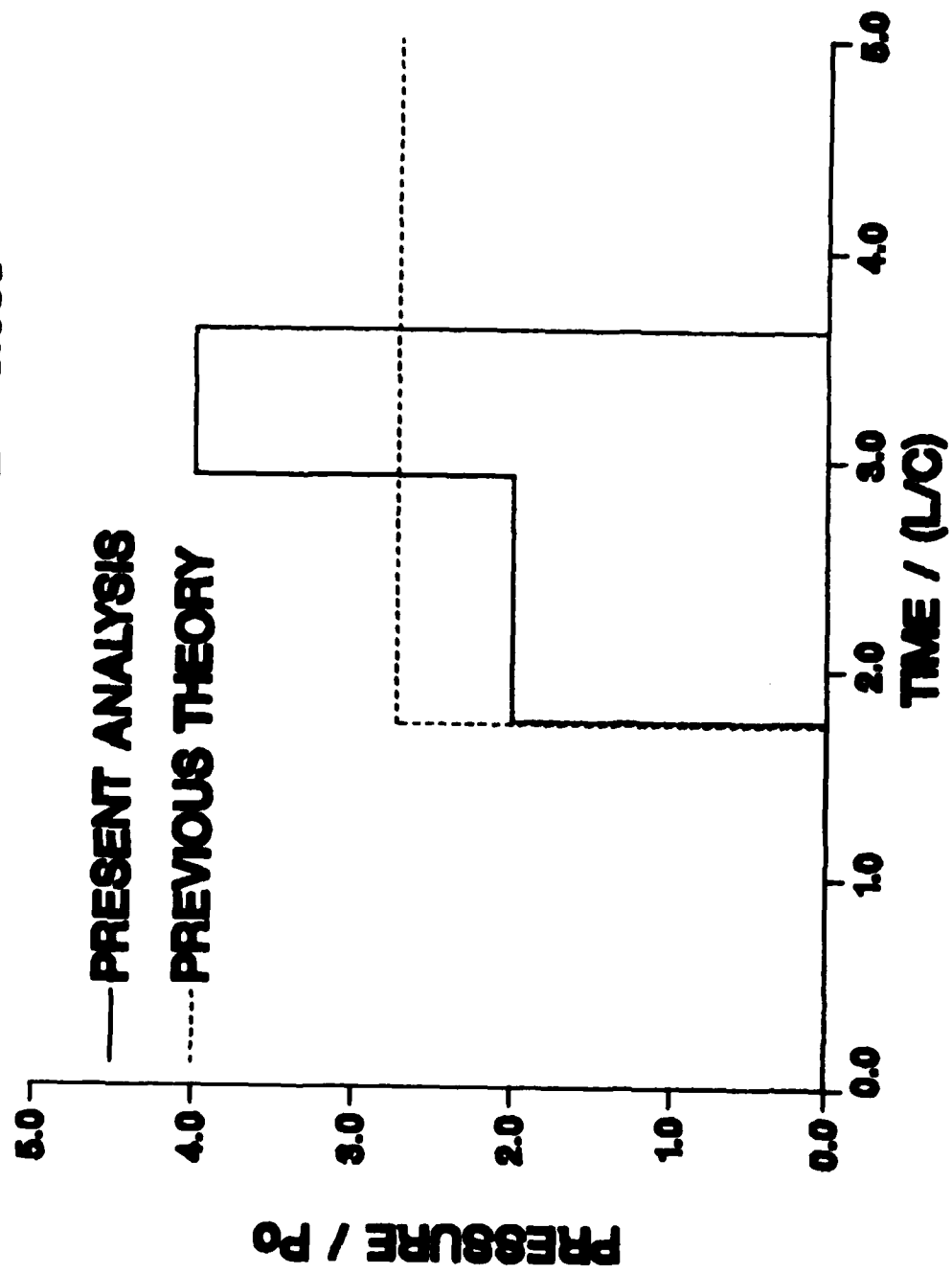


Figure 22. Endwall Pressure versus Time, Fill Ratio = .95, $P_0/E = .035$

ENDWALL PRESSURE VERSUS TIME

FILL RATIO = 0.830 $P_0 / E = 0.035$

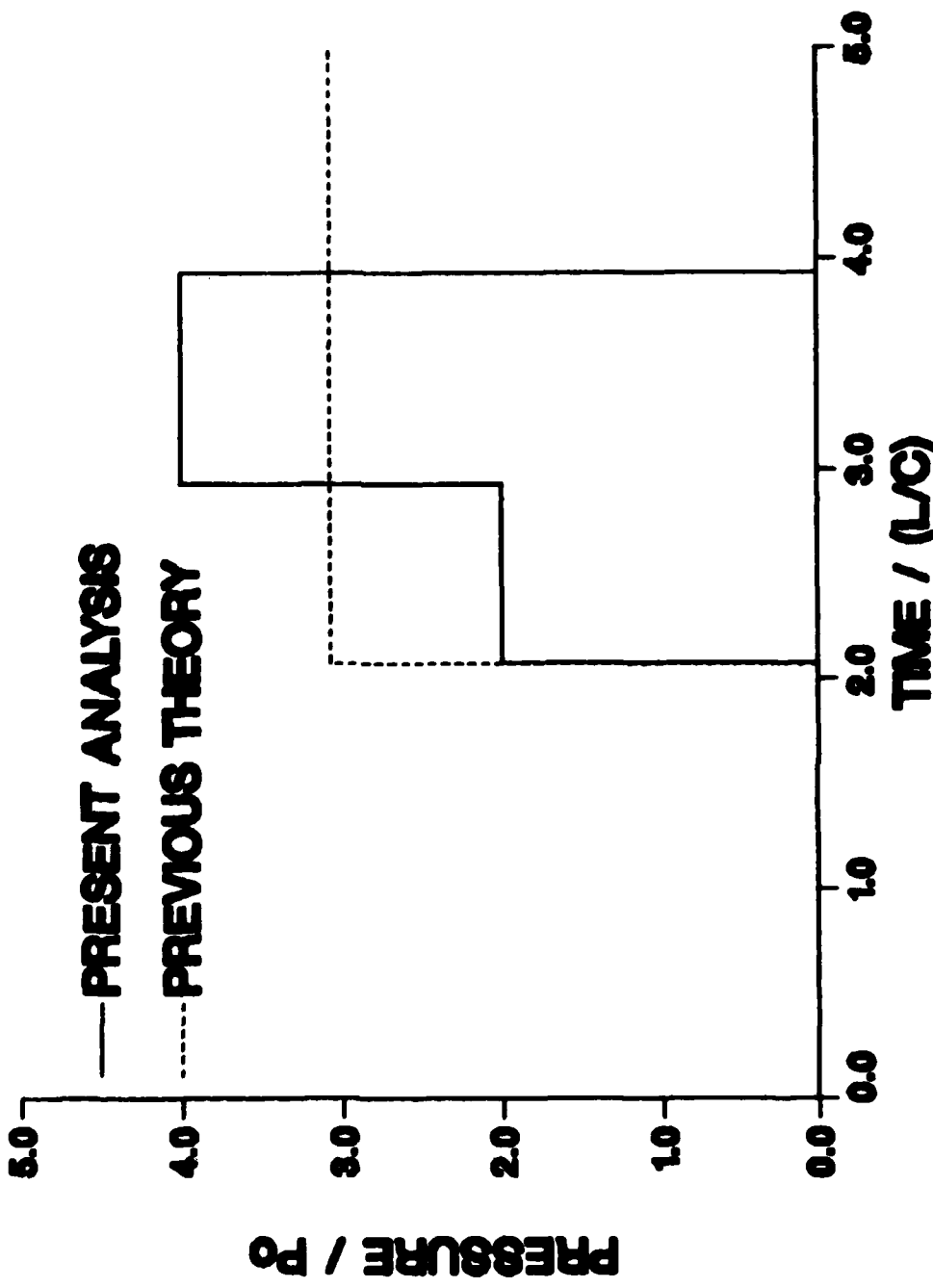


Figure 23. Endwall Pressure versus Time, Fill Ratio = .93, $P_0/E = .035$

ENDWALL PRESSURE VERSUS TIME

FILL RATIO = 0.800 $P_0 / E = 0.035$

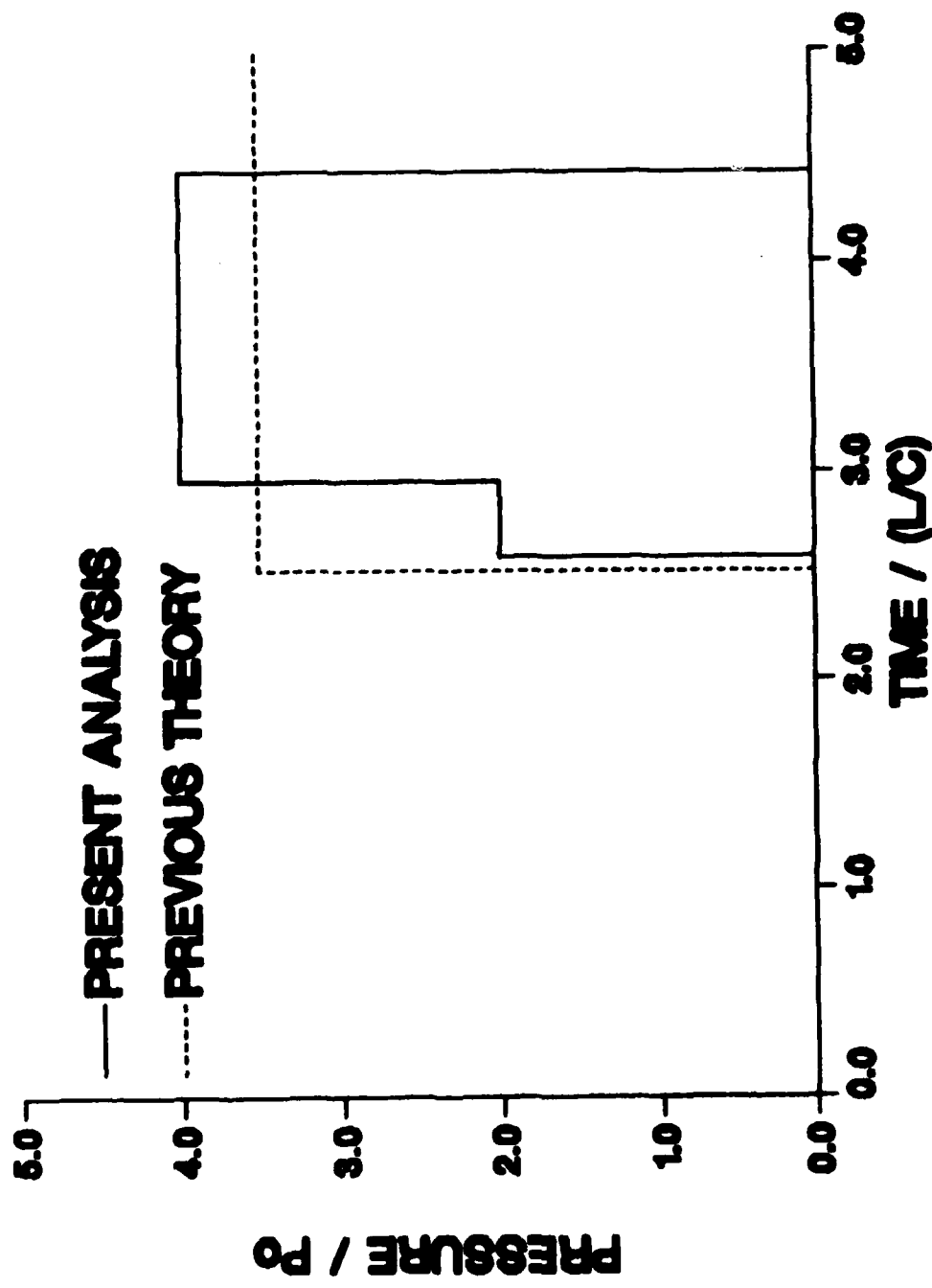


Figure 24. Endwall Pressure versus Time, Fill Ratio = .90, $P_0/E = .035$

ENDWALL PRESSURE VERSUS TIME

FILL RATIO = 0.950 $P_0 / E = 0.025$

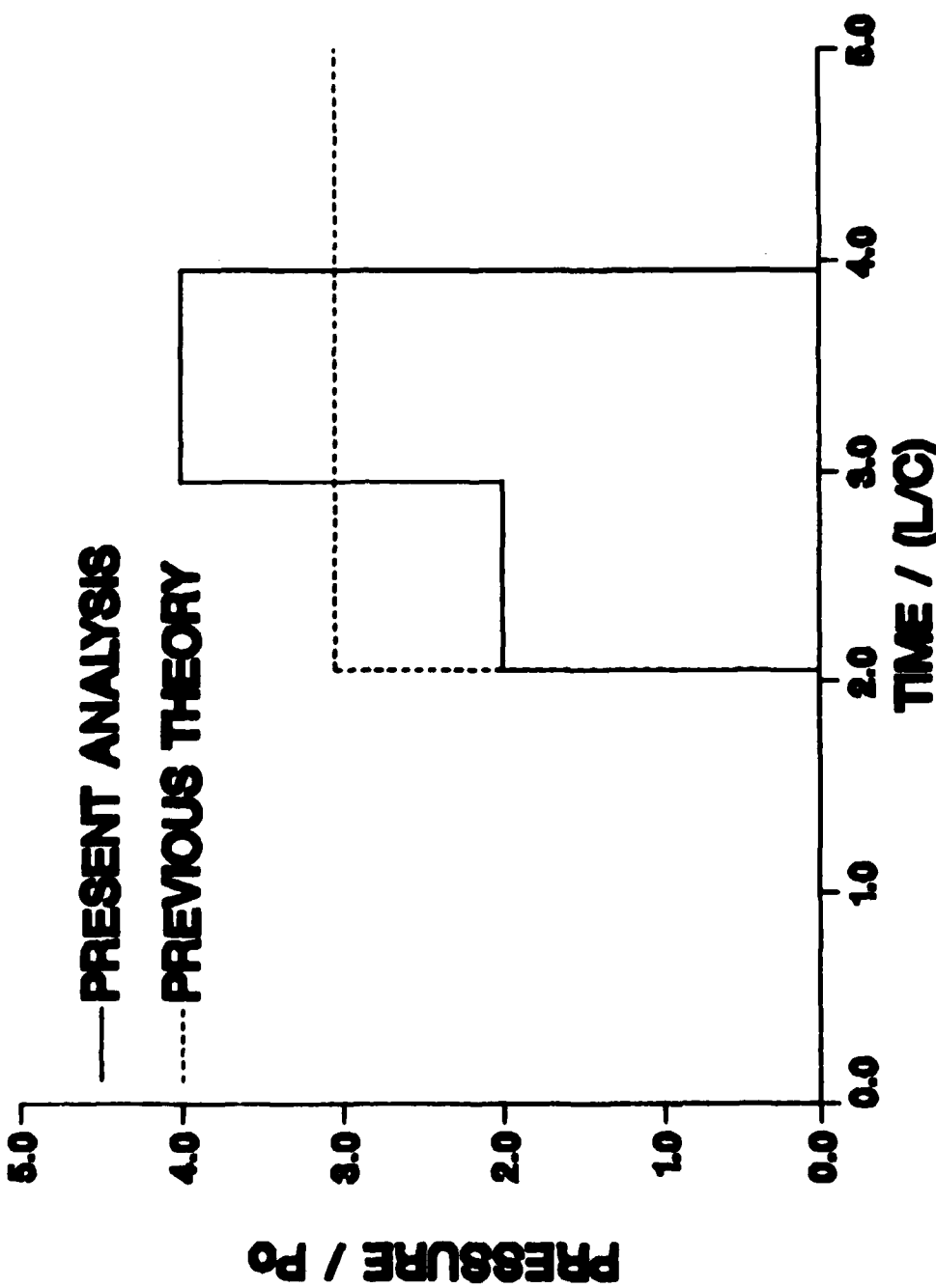


Figure 25. Endwall Pressure versus Time, Fill Ratio = .95, $P_0/E = .025$

ENDWALL PRESSURE VERSUS TIME

FILL RATIO = 0.950 $P_0 / E = 0.035$

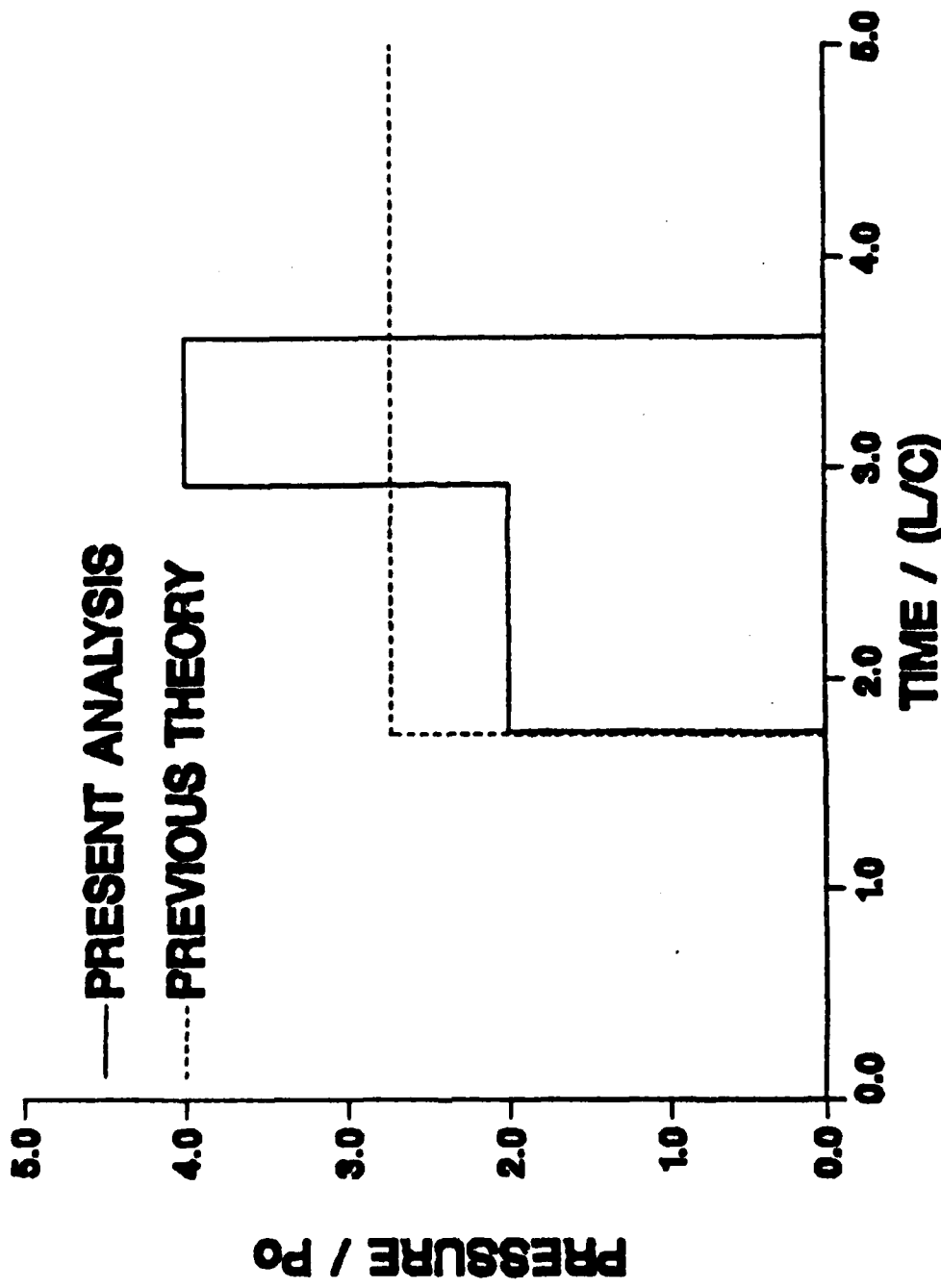


Figure 26. Endwall Pressure versus Time, Fill Ratio = .95, $P_0/E = .035$

ENDWALL PRESSURE VERSUS TIME

Fill Ratio = 0.850 $P_o / E = 0.050$

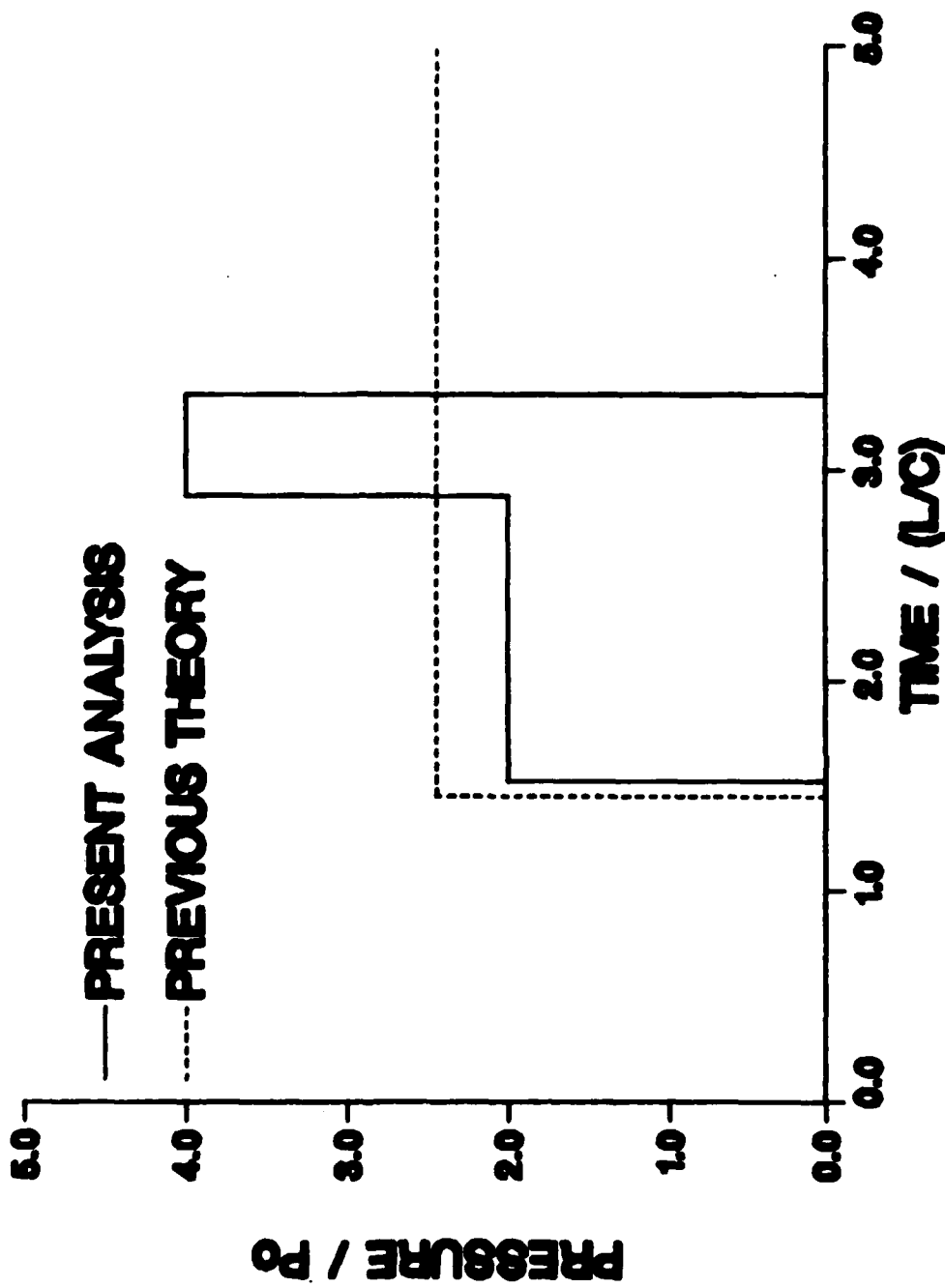


Figure 27. Endwall Pressure versus Time, Fill Ratio = .95, $P_o/E = .05$

ENDWALL PRESSURE VERSUS TIME

FILL RATIO = 0.950 $P_0 / E = 0.100$

PRESENT ANALYSIS

PREVIOUS THEORY

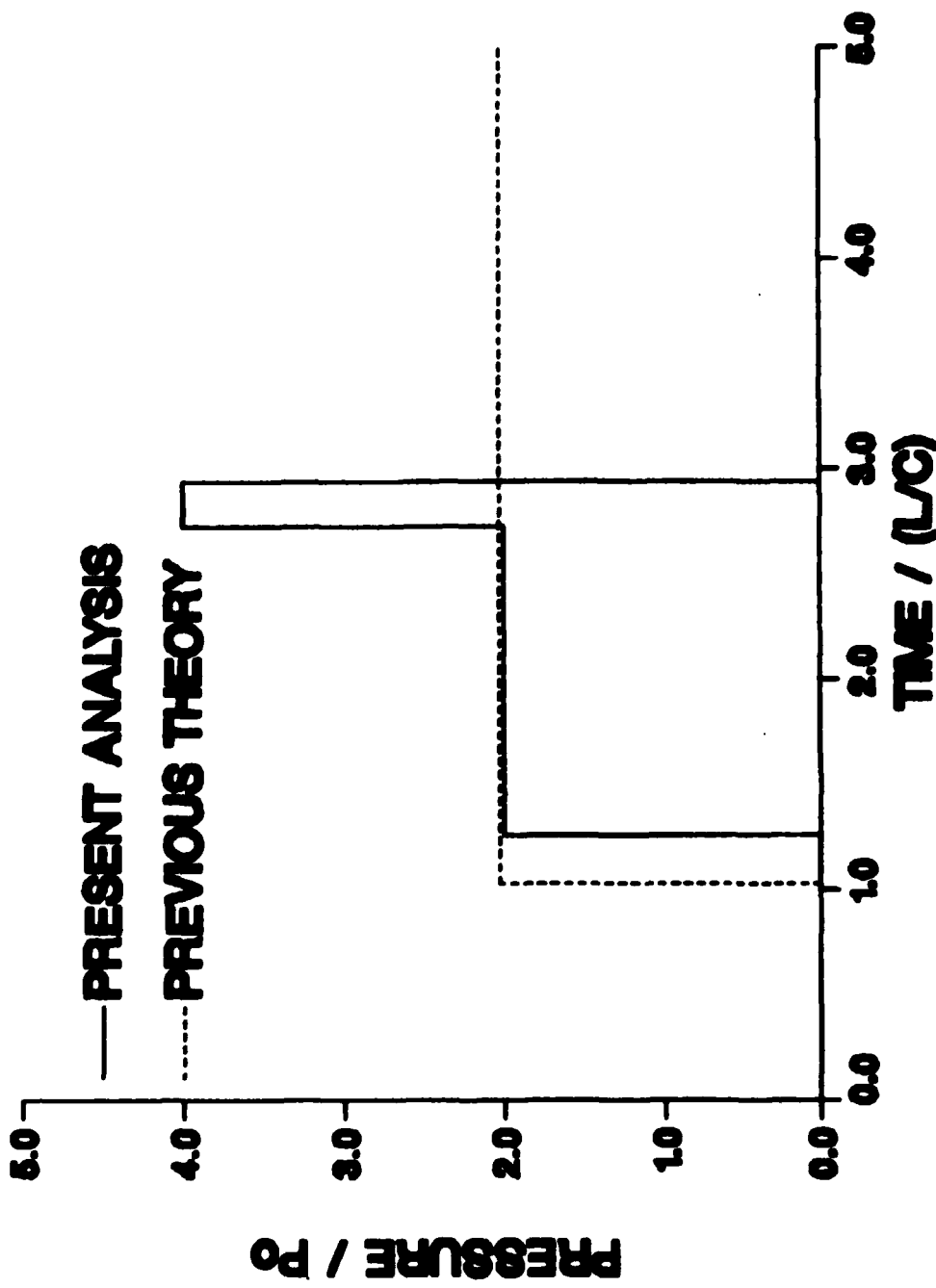


Figure 28. Endwall Pressure versus Time, Fill Ratio = .95, $P_0/E = .10$

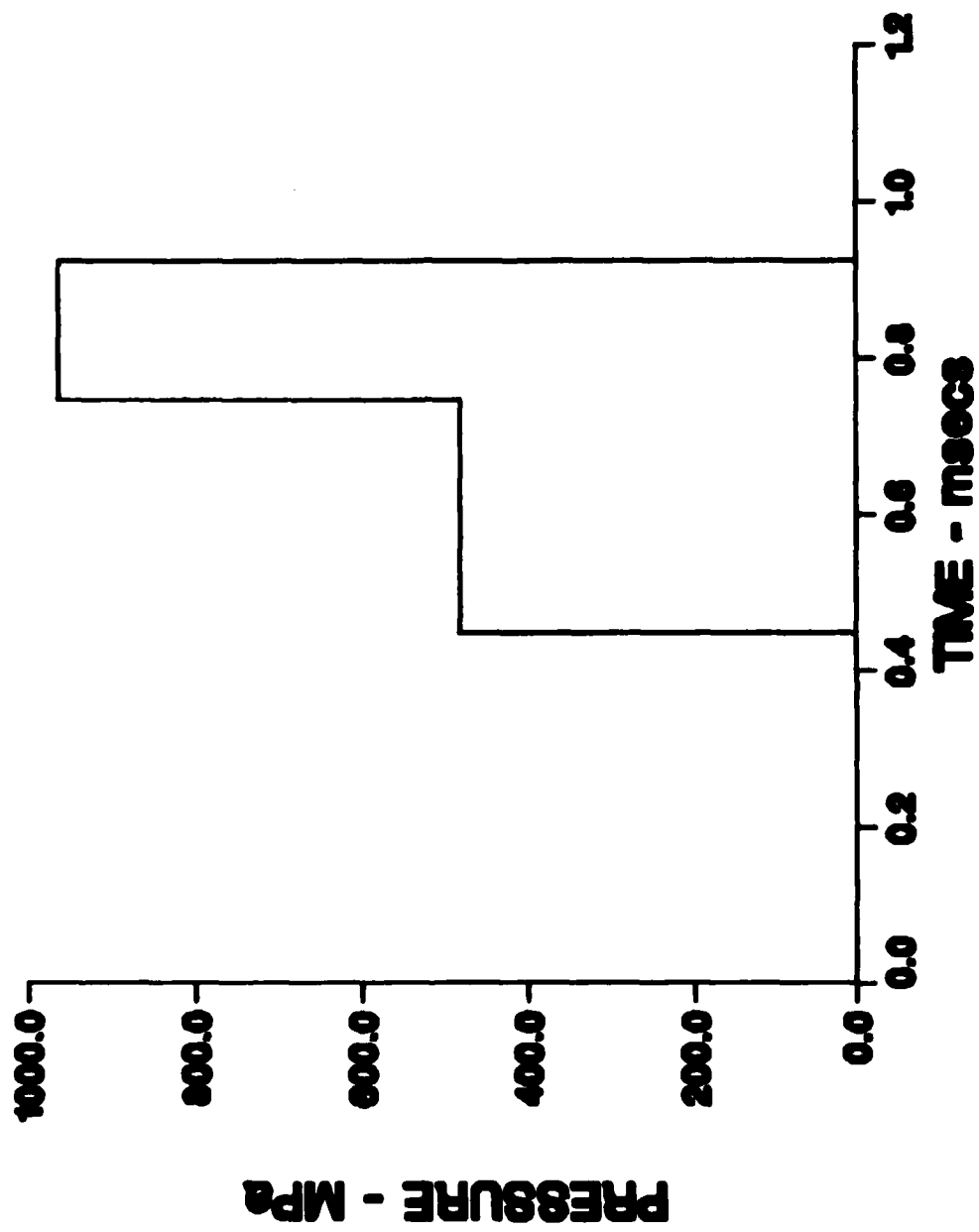


Figure 29. Endwall Pressure versus Time, Dimensional Result

LIST OF SYMBOLS

c	speed of sound in fluid, m/s
E	bulk modulus of fluid, N/m ²
L	length of fluid slug, m
H	length of cylinder, m
P	local pressure, N/m ²
P _{BOUNDARY}	pressure at liquid interface, N/m ²
P ₀	magnitude of initial pressure step, N/m ²
V	local velocity, m/s
V ₀	velocity behind initial compression wave, m/s
x	nondimensional distance from bottom of cylinder, m
x'	distance from bottom of cylinder, m
ρ	local fluid density, kg/m ³

DISTRIBUTION LIST

<u>No. of Copies</u>	<u>Organization</u>	<u>No. of Copies</u>	<u>Organization</u>
12	Administrator Defense Technical Info Center ATTN: DTIC-DDA Cameron Station Alexandria, VA 22304-6145	1	Director US Army Air Mobility Research and Development Laboratory Ames Research Center Moffett Field, CA 94035
1	HQDA DAMA-ART-M Washington, DC 20310	1	Commander US Army Communications- Electronics Command ATTN: AMSEL-ED Fort Monmouth, NJ 07703
1	Commander US Army Materiel Command ATTN: AMCDRA-ST 5001 Eisenhower Avenue Alexandria, VA 22333-0001	1	Commander ERADOM Technical Library ATTN: DELSD-L (Reports Section) Fort Monmouth, NJ 07703-53001
3	Commander Armament R&D Center US Army AMCCOM ATTN: SMCAR-TDC SMCAR-TSS SMCAR-LCA-F Mr. D. Mertz Mr. E. Falkowski Mr. A. Loeb Mr. R. Kline Mr. S. Kahn Mr. H. Hudgins Dover, NJ 07801	3	Commander US Army Missile Command ATTN: AMSMI-R AMSMI-RDK Dr. Bill Walker Mr. R. Deep Redstone Arsenal, AL 35898
1	Commander US Army Armament, Munitions and Chemical Command ATTN: SMCAR-ESP-L Rock Island, IL 61299	1	Commander US Army Missile Command ATTN: AMSMI-YDL Redstone Arsenal, AL 35898
1	Director Benet Weapons Laboratory Armament R&D Center US Army AMCCOM ATTN: SMCAR-LCB-TL Watervliet, NY 12189	1	Commander US Army Tank Automotive Command ATTN: AMSTA-TSL Warren, MI 48090
1	Commander US Army Aviation Research and Development Command ATTN: AMSAV-E 4300 Goodfellow Blvd St. Louis, MO 63120	1	Director US Army TRADOC Systems Analysis Activity ATTN: ATAA-SL White Sands Missile Range, NM 88002
		1	Commander US Army Research Office P. O. Box 12211 Research Triangle Park, NC 27709-2211



DISTRIBUTION LIST

<u>No. of Copies</u>	<u>Organization</u>	<u>No. of Copies</u>	<u>Organization</u>
1	Commander US Naval Air Systems Command ATTN: AIR-604 Washington, DC 20360	1	AFWL/SUL Kirtland AFB, NM 87117
2	Commander David W. Taylor Naval Ship Research and Development Center ATTN: Dr. S. de los Santos Mr. Stanley Gottlieb Bethesda, Maryland 20084	1	Air Force Armament Laboratory ATTN: AFATL/DLODL Eglin AFB, FL 32542-5000
2	Commander US Naval Surface Weapons Center ATTN: Code DK20 Dr. F. Moore Dahlgren, VA 22448	1	Massachusetts Institute of Technology ATTN: Tech Library 77 Massachusetts Avenue Cambridge, MA 02139
1	Commander US Naval Surface Weapons Center ATTN: Dr. U. Jettmar Silver Spring, MD 20910	1	Virginia Polytechnic Institute & State University ATTN: Dr. Clark H. Lewis Department of Aerospace & Ocean Engineering Blacksburg, VA 24061
1	Commander US Naval Weapons Center ATTN: Tech Svcs Br., Code 3433 China Lake, CA 93555	1	University of Delaware Mechanical and Aerospace Engineering Department ATTN: Dr. J. E. Danberg Newark, DE 19711
1	Commander US Army Development & Employment Agency ATTN: MODE-TED-SAB Fort Lewis, WA 98433	3	Sandia National Laboratories ATTN: Technical Staff Dr. W. L. Oberkampf Aeroballistics Division 5631, H. R. Vaughn Dr. F. Blottner Albuquerque, NM 87184
1	Director NASA Langley Research Center ATTN: NS-185, Tech Lib Langley Station Hampton, VA 23365	<u>Aberdeen Proving Ground</u>	
1	Commandant US Army Infantry School ATTN: ATSH-CD-CSO-OR Fort Benning, GA 31905	Dir, USAMSAA ATTN: AMXSY-D AMXSY-MP, H. Cohen	
		Cdr, II ^{IC} TECOM ATTN: TE-TO-F	
		Cdr, CRDC, AMCCOM ATTN: SMCCR-RSP-A SMCCR-MU SMCCR-SPS-IL	

USER EVALUATION SHEET/CHANGE OF ADDRESS

This Laboratory undertakes a continuing effort to improve the quality of the reports it publishes. Your comments/answers to the items/questions below will aid us in our efforts.

1. BRL Report Number _____ Date of Report _____

2. Date Report Received _____

3. Does this report satisfy a need? (Comment on purpose, related project, or other area of interest for which the report will be used.)

4. How specifically, is the report being used? (Information source, design data, procedure, source of ideas, etc.)

5. Has the information in this report led to any quantitative savings as far as man-hours or dollars saved, operating costs avoided or efficiencies achieved, etc? If so, please elaborate.

6. General Comments. What do you think should be changed to improve future reports? (Indicate changes to organization, technical content, format, etc.)

CURRENT ADDRESS Name _____
 Organization _____
 Address _____
 City, State, Zip _____

7. If indicating a Change of Address or Address Correction, please provide the New or Correct Address in Block 6 above and the Old or Incorrect address below.

OLD ADDRESS Name _____
 Organization _____
 Address _____
 City, State, Zip _____

(Remove this sheet along the perforation, fold as indicated, staple or tape closed, and mail.)

----- FOLD HERE -----

Director
US Army Ballistic Research Laboratory
ATTN: AMXBR-OD-ST
Aberdeen Proving Ground, MD 21005-5066

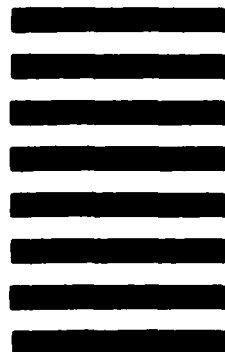


NO POSTAGE
NECESSARY
IF MAILED
IN THE
UNITED STATES

OFFICIAL BUSINESS
PENALTY FOR PRIVATE USE. \$300

BUSINESS REPLY MAIL
FIRST CLASS PERMIT NO 12062 WASHINGTON, DC
POSTAGE WILL BE PAID BY DEPARTMENT OF THE ARMY

Director
US Army Ballistic Research Laboratory
ATTN: AMXBR-OD-ST
Aberdeen Proving Ground, MD 21005-9989



----- FOLD HERE -----

END

FILMED

11-85

DTIC